ISSN : 2320 - 2122

JAN 2013
Vol.I , IssueII

સર્જન

SARJAN

SOCET Journal

Silver Oak College of Engineering & Technology
Ahmedabad

ISSN:2320 - 2122 Vol I, Issue II January 2013

SARJAN

Engineering & Technology Journal,

Silver Oak College of Engineering & Technology

Silver Oak College of Engineering & Technology, Opp. Bhagwat Vidhyapith ,

Nr. Gota Cross road, Ahmedabd-382481

Web site: www.socet.edu.in

MESSAGE FROM Prof. (Dr.) M.N.Patel

Prof. (Dr.) M. N. Patel
Principal,
L. D. College of Engineering
Member Secretary,
Admission Committee for Professional Courses
Director,
Gujarat Technological University

On the occasion of the publication of "Sarjan" - a technical journal of Silver Oak College of Engineering and Technology, I would like to send my warmest congratulations and good wishes and would like to communicate few words with the technology aspirants. Your work is going to fill a large part of your life, and the only way to be truly satisfied is to do what you believe is great work. And the only way to do great work is to love what you do. If you haven't found it yet, keep looking. Don't settle. As with all matters of the heart, you'll know when you find it. And, like any great relationship, it just gets better and better as the years roll on. So keep looking until you find it. Don't settle.

SOCET has done and continues to perform a most excellent service to the fraternity of knowledge seeker in the field of engineering. I have also noted with great pleasure that the institute has consistently increased its scope of activities and perform at most commendable standards.

I hope that "SARJAN" will bridge the gap between the theory and practice of technology.

With affectionate thoughts.

Prof. (Dr.) M. N. Patel

MESSAGE FROM Dr. D.J.SHAH

Dr. Dharmesh J. Shah

Principal ,

LCIT, Bhandu

Dean,

Engineering (Zone II), GTU, Ahmedabad

I am delighted to introduce the 2nd issue of the technical journal "SARJAN". Research plays pivotal role in the engineering education. Dissemination of knowledge acquired through research among the researchers is equally important. "SARJAN" will help to explore the new avenues of innovations among the faculties, help them to move forward in their ongoing research and also help society to improve the quality of education & research in the field of engineering & technology.

Dr. Dharmesh J. Shah

E D I T O R I A L

Dr. P.K.Shah,
Dean,
Silver Oak College of Engg. & Tech.,
Ahmedabad

"SARJAN" is on the way of progress. We are very happy that the 1st issue of 'SARJAN' has received an overwhelming response from Professors, students and experts in the field of technical education. This has inspired us to make this Journal more knowledgeful with latest research and quality papers. This 2nd issue is coming up with such selected papers. We are sure that the learned readers will heartily accept our serious efforts. We are very glad to announce that our Journal is recognized and registered by ISSN and they have assigned our Journal an ISSN number.

At this juncture, I am very much thankful to Prof. (Dr.) M. N. Patel who has appreciated our SOCET Journal and conveyed his inspiring message. I am equally thankful to Dr. D. J. Shah for his valuable message. My sincere thank goes to our Chairman Sir Shri Shitalbhai Agrawal, our Executive Director Sir Shri Janakbhai Khandwala, our Principal Sir Shri Saurin Shah and our academic Director Sir Shri Ravikumar who are always with us to support at any time. I thank all the authors who have contributed their research work. I thank my editorial team Professors who are continuously working hard for bringing up this Journal in time.

We hope this Journal will be beneficial to people in technical field and to the society. We invite your suggestions to make this Journal more qualitative.

Dr. P. K. Shah,
Editor

Co-ordinators,
Prof. J. K. Shah
Prof. R. D. Makwana
Prof. I. B.Thakar
Prof. A. R. Agarawal

In This Issue

ISSN:2320 – 2122 Vol. I, Issue II January 2013

Dynamic Characterization Of End Milling Machine Components

Khushbu Patel
Asst.Prof.,Mechanical Engg.Dept, Silver Oak College of Engg.&Technology, Ahmedabad, Gujarat, India
khush_10@yahoo.co.in

***Abstract*- Dynamic excitation of any machine tool structure is based on natural frequency of the structure and corresponding mode shape. Initial work of the thesis presents a systematic procedure and details of the use of experimental analysis and finite element modal analysis technique for determining the structural dynamic response of end milling machine.The simplified experimental modal analysis of different components of milling machine is carried out with FFT analyzer to obtain the actual natural frequencies of the individual component of milling machine. CAD model of the machine tool's structure is made by using design software SOLIDWORKS and analyzed by finite element simulation using ANSYS software.The findings of an experimental study conducted on milling machine, is investigated. The ANSYS results of modal analysis and modal analysis shows good agreement with the experimental results captured using FFT analyzer.**

***Keywords*- FEA, Modal Analysis**

I INTRODUCTION

Milling is a machining process in which metal is removed by a rotating multiple-tooth cutter. As the cutter rotates, each tooth removes a small amount of material from the advancing work for each spindle revolution. The relative motion between work piece and cutter can be in any direction. Surfaces having any orientation can be machined in milling. What distinguishes milling from other machining processes are interrupted cutting, relatively small size of chips and variation of chip thickness within a chip itself.

If a linear approximation of the machine structure is made, the machine response to any dynamic excitation may be estimated based on its Natural Frequencies and Corresponding Mode Shapes. These, may be acquired either from a theoretical computation of Finite Element Analysis (FEA), or from an Experimental Modal Analysis (EMA).

1.1 Significance Of Modal Analysis

Modal analysis is a process whereby a structure may be defined in terms of its natural characteristics which are the frequency, damping, and mode shapes—its dynamic properties.

These natural frequencies and mode shapes occur in all structures that we design. Basically, there are characteristics that depend on the weight and stiffness of structure which determine where these natural frequencies and mode shapes will exist. As a design engineer, one should need to identify these frequencies and know how they might affect the response of a structure, when a force excites the structure. Understanding the mode shape and how the structure will vibrate when exited, helps the design engineer to design better structure.

1.1.1 Basic Concept Related To Modal Analysis

Mode is the manifestation of energy which is trapped within the boundaries of the structure, and cannot readily escape. Modes are further characterized as either rigid body or flexible body modes. All structure can have up to six rigid body modes, three translational and three rotational on microscopic scale.

Each mode is defined by a natural (or modal) frequency, a value of damping, and a mode shape. Modes are the properties of structure, and are independent of the type of excitation force used to excite it.

1.2 Dynamic Analysis

When a structure has a loading which varies with time, it is reasonable to assume its response will also vary with time. In such cases, a dynamic analysis may have to be performed which reflects both the varying load and response. If however, the frequency of loading is low compared with the natural frequency of loading is low compare with the natural frequency of the structure, then the response given by a static analysis under the instantaneous law may suffice. This assumption is normally applied when the frequency is less than one third of lowest natural frequency. If the applied load varies rapidly, then a variety of solution technique may be employed which take into account inertial effects due to mass and damping effects.

II METHODOLOGY

2.1 Specification Of Vertical Milling Machine

TableLength,width,height: 1700mm×310mm×88mm
Column height : 1800mm
Column width : 500mm
Spindle diameter : 150mm
Spindle speed (minimum) : 32 rpm

Spindle speed (maximum) : 1400 rpm
Distance between spindle centre and inner column: 400mm
Distance between spindle centre and outer column: 200mm
Inner guide way: 65mm
Outer guide way: 140mm
Permissible Up and down movement of table: 450mm
Permissible Spindle movement: 80mm

Table 1 Material Properties of Various Part of Milling Machine

Material Properties of Various Part of Milling Machine	
Machine tool body	High grade cast iron treated with artificial aging
Spindle	Chrome and molybdenum alloy
Nut	High grade phosphor bronze
Base	Grey cast iron
Table	Cast iron
Saddle	Cast iron
Milling cutter	High speed steel
Work piece	Mild steel

2.2 Performance Of Experiment

The milling machine will be tested in this work is performed using a modal analysis test, in which the force hammer is used to impact on different points and the resultant vibrations will be measured in one point. Frequency response function (FRF) is measured. From the data of speed and capacity of machine tool the displacement/ frequency can also measured.

2.3 FFT Analyzer

Fourier's basic theorem states that any waveform in the time domain can be represented by the weighted sum of pure sine waves of all frequencies. If the signal in the time domain (as viewed on an oscilloscope) is periodic, then its spectrum is probably dominated by a single frequency component. What the spectrum analyzer does is represent the time domain signal by its component frequencies. For one thing, some measurements which are very hard in the time domain are very easy in the frequency domain. Take harmonic distortion. It's hard to quantify the distortion by looking at a good sine wave output from a function generator on an oscilloscope. When the same signal is displayed on a spectrum analyzer, the harmonic frequencies and amplitudes are displayed with amazing clarity.

FFT stands for Fast Fourier Transform. The FFT is a faster version of the Discrete Fourier Transform (DFT). The DFT is extremely important in the area of frequency (spectrum) analysis because it takes a discrete signal in the time domain and transforms that signal into its discrete frequency domain representation. Without a discrete-time to discrete-frequency transform we would not be able to compute the Fourier transform The FFT utilizes some clever algorithms to do the same thing as the DTF, but in much less time. Fig. 1 shows FFT Analyzer used for experimental results.

Due to the Complexity of structure of the milling machine, it is a difficult thing to build the finite element modeling of the whole machine tool structure. Therefore the machine tool is broken down into several fundamental parts, such as the upright columns, the cross beam, the slide carriage and spindle which is modeled with design software SOLID WORKs.

Fig. 1 VibXpert FFT Analyzer

2.4 Creation Of Finite Element Model

The goal of mesh design is to select the number and location of finite-element nodes and element types so that the associated analyses are sufficiently accurate. Several methods include automatic-mesh generation with adaptive capabilities, which serve to produce and iteratively refine the mesh based on a user-selected error tolerance. In problems without severe stress concentrations, much of the mesh data can be developed conveniently using automatic mesh generation. With the input file developed, the analysis processor is activated and raw output files are generated.

Meshed body of milling machine under consideration is shown in Fig. 2

The finite element modeling is carried out with ANSYS, using solid element with 10 node tetrahedral and three degree of freedom per node with a total of 10125 elements and 19097 nodes. The materials of all parts are considered as defined in earlier section the Chrome and molybdenum alloy material with the following properties: Young's modulus is 4.5×1010 Pa; Shear Modulus 1.6667×1010 Pa; density is 1800 kg/m3; Poisson ratio is 0.35; Bulk modulus 5×1010 Pa; Gray cast iron with the following properties: Young's

modulus is 1.1×1010 Pa; Shear Modulus 4.296×1010 Pa; density is 7200 kg/m3; Poisson ratio is 0.28; Bulk modulus 8.333×1010Pa; steel with the following properties: Young's modulus is 2×1011 Pa; Shear Modulus 7.692×1010 Pa; density is 7850 kg/m3; Poisson ratio is 0.3; Bulk modulus 1.6667×1011 Pa.

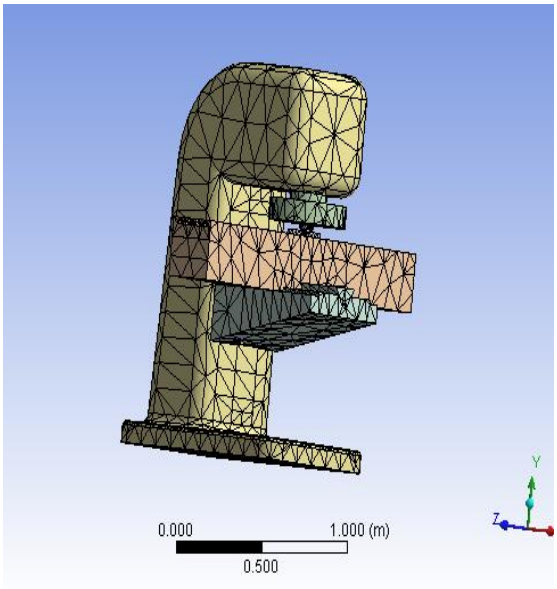

Fig. 2 Meshed model of milling machine

2.5 Modal Analysis

As discussed in previously Experimental results are carried out with FFT analyzer of milling spindle, table and saddle. From that we have found natural frequency of each component experimentally then by modal analysis comparison of both derived frequency is done.

Modal analysis of milling spindle is carried out with defined boundary condition. Fig. 3 shows the separate cad model of milling spindle.

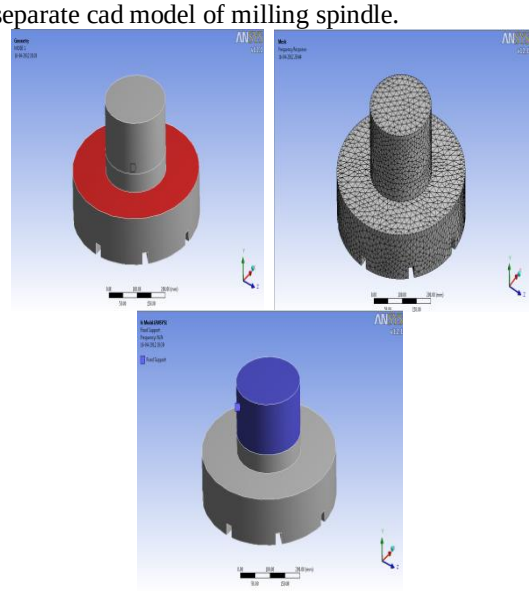

Fig. 3 CAD model of Spindle and Meshing of Spindle with Applied Boundary Condition

Fig. 4 shows the ANSYS results of milling spindle with mode 1 which gives the frequency of 17.275, Fig. 7 shows the ANSYS results of table with mode 2 gives the frequency of 19.102, and Fig. 8 shows the ANSYS results of table with mode 3 gives the frequency of 19.123.

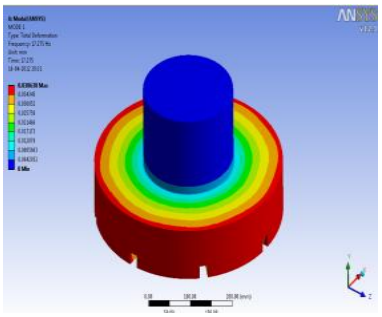

Fig. 4 Schematic view of milling table at mode 1

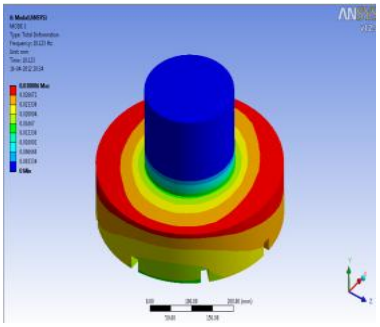

Fig. 5 Schematic view of milling table at mode 2

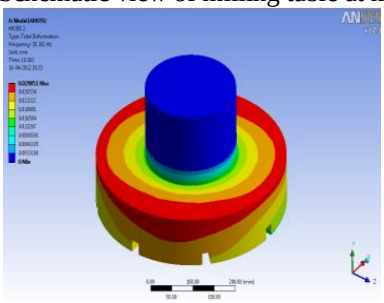

Fig. 6 Schematic view of milling table at mode 3

Experimental results are taken by FFT analyzer, table 2 shows amplitude and frequency value for milling spindle obsered from FFT analyzer at without rotation condition

Table 2 Experimental results of amplitude and frequency of milling spindle

Amplitude (Velocity mm/s)	Frequency (Hz)
0.027	2.00
0.042	17.00
0.016	19.00
0.005	25.00

Table 3 shows the comparisons of experimental results and ANSYS result frequency

of milling spindle. We can see that simulated ANSYS results are very close to experimental results. For both modes 2 and mode 3 ANSYS results are near 19 Hz so we can say that spindle is having natural frequency of 19 Hz.

Modal analysis of milling table is carried out with defined boundary condition of fixed support which is provided at contact region of table with saddle. Fig. 7 shows the separate cad model of milling table.

Table 3 Comparison of value of frequency values for milling spindle in steady position

Comparisons of natural frequencies of spindle (Hz)			
Sr. No.	**Experimental results**	**ANSYS results**	**Error (%)**
1	17	17.275	1.61
2	19	19.102	0.5368
3	19	19.123	0.64

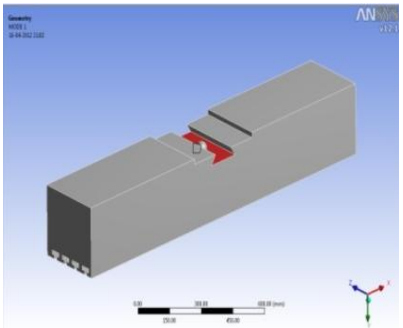

Fig. 7 CAD model of milling table

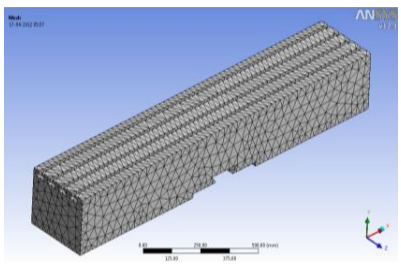

Fig. 8 Meshed Model of milling table

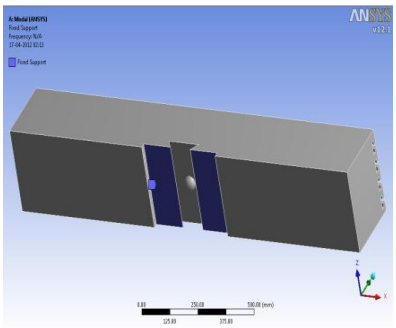

Fig. 9 Milling Table Model with applied boundary condition

Fig. 8 shows meshed model of milling table, Type of Meshing used is 3D meshing; Type of Element used is 10 Node Tetrahedral; Number of Nodes are 11409; Number of Elements are 6178.

Fig. 10 shows the ANSYS results of milling table with mode 1 which gives the frequency of 13.564, Fig. 13 shows the ANSYS results of milling table with mode 2 gives the frequency of 16.522, and Fig. 14 shows the ANSYS results of milling table with mode 3 gives the frequency of 18.66.

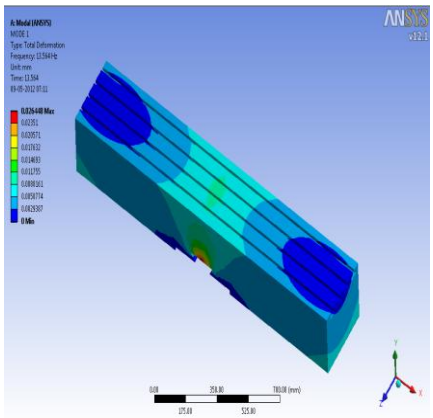

Fig. 10 Schematic view of milling table model at Mode1

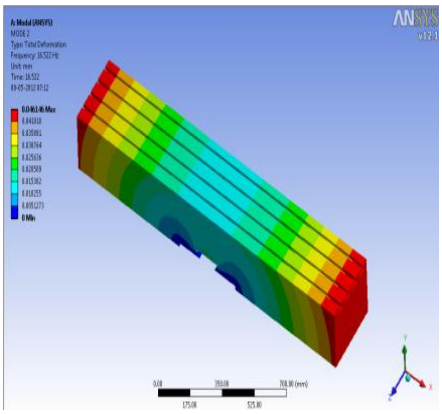

Fig. 11 Schematic view of milling table model at Mode2

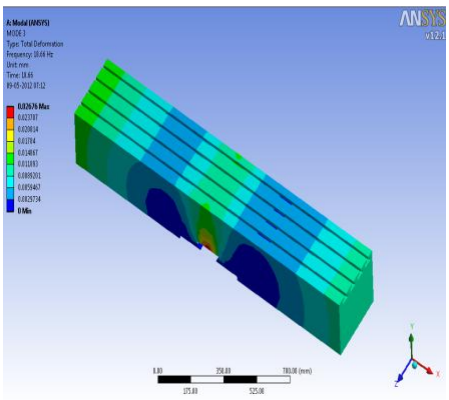

Fig. 12 Schematic view of milling table model at Mode3

Table 4 shows amplitude and frequency value for milling table observed from FFT analyzer at without rotation condition.

Table 4 Experimental results amplitude and frequency values for milling table in steady position of milling table

Amplitude (Velocity) (mm/s)	Frequency (Hz)
0.027	11.90
0.024	14.00
0.011	18.00
0.016	24.00

Table 5 shows the comparisons of experimental results and ANSYS result frequency of milling table. We can see that simulated ANSYS results are close to experimental results.

Table 5 Comparison of value of frequencyof milling table in steady position

Comparisons Of Natural Frequencies Of Table (Hz)			
Sr. No.	Experimental Results	ANSYS Results	Error (%)
1	11.9	13.564	13.98
2	14	16.522	18.01
3	18	18.66	3.66

Modal analysis of milling saddle is carried out with defined boundary condition of fixed support which is provided at contact region of saddle with milling vertical column. Fig. 13 shows the separate cad model of milling saddle.

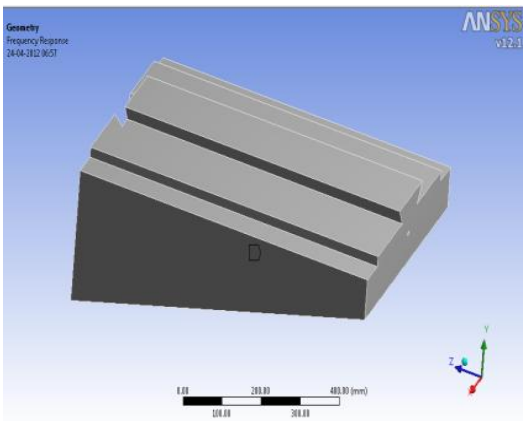

Fig. 13 CAD model of milling saddle

Fig. 14 shows meshed model of milling saddle. Type of Meshing used is 3D meshing; Type of Element is 10 node Tetrahedral; Number of Nodes are 3358; Number of Elements are 1824.

Fig. 16 shows the ANSYS results of table with mode 1 which gives the frequency of 11.292 Hz, Fig. 17 shows the ANSYS results of table with mode 2 gives the frequency of 12.113 Hz.

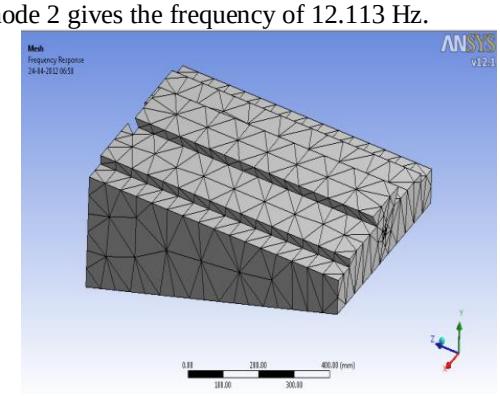

Fig. 14 Meshed Model of milling saddle

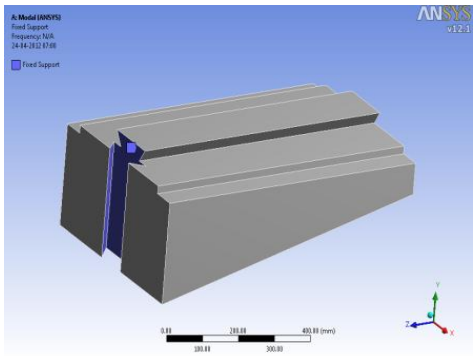

Fig. 15 Saddle Model with Applied saddle

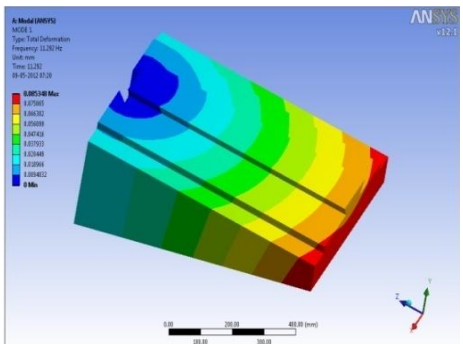

Fig. 16 Schematic view of milling saddle at Mode1

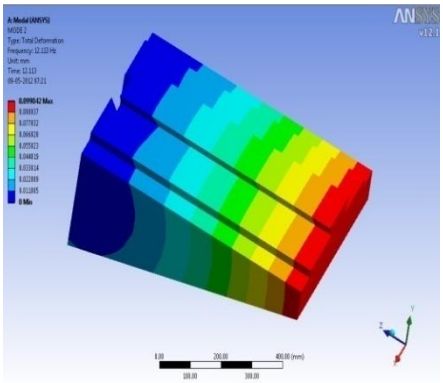

Fig. 17 Schematic view of milling saddle at Mode2

Table 6 shows amplitude and frequency value for milling saddle observed from FFT analyzer at without rotation condition.

Table 6 Experimental results amplitude and frequency value of milling saddle in steady position

Amplitude (velocity mm/s)	Frequency (Hz)
0.022	11.00
0.016	15.00
0.053	19.00
0.008	26.00

Table 7 shows the comparisons of experimental results and ANSYS result frequency of milling spindle. We can see that simulated ANSYS results are nearly close to experimental results.

Table 7 Comparison of results

Comparisons Of Natural Frequencies (Hz)			
Sr. No.	Experimental results	ANSYS results	Error (%)
1	11	11.292	2.65
2	15	12.113	19.246

III CONCLUSION

A comparison of calculated modes with their measured counterparts is very helpful in general to verify the quality of a finite element model for dynamic simulation purposes and to detect any possible improvements. Experimental modal analysis is performed for validating the results obtained by ANSYS.

The comparison between natural frequencies of finite element modeling and model testing shows the closeness of the results. This research work will help to find out the natural frequencies of the machine and hence predicting the dynamic characterization of machine tool.

REFERENCES

[1]Anayet U. Patwari, Waleed F. Faris, A. K. M. Nurul Amin, and S. K. Loh,"Dynamic Modal Analysis of Vertical Machining Centre Components'' Hindawi Publishing Corporation Advances in Acoustics and Vibration,2009

[2]J. Rotberg , B. Bork "Structural Dynamic Behaviour of a High-Speed Milling Machine''

[3]Jui P. Hung, Yuan L. Lai, Hui, T. You "Finite Element Prediction on the Machining Stability of Milling Machine with Experimental Verification'' World Academy of Science, Engineering and Technology 72- 2010

[4]R. Sagherian and M.A. Elbestawi, "a simulation system for improving machining accuracy in milling machine'' Elsevier Science Publishers B.V.,1990

[5]Neville F. Rieger "the Relationship between Finite Element Analysis and Modal Analysis'' Stress Technology Incorporated, Rochester, New York.

[6]S. V. Modak, T. K. Kundra and B. C. Nakra "use of an updated finite element model for dynamic design"
S. V. modak, T. K. kundra, and B. C. Nakra "prediction of dynamic characteristics using updated finite element models'' Department of Mechanical Engineering, Indian Institute of Technology, Hauz Khas, New Delhi, 110016, India.

[7]S. V. Modak, T. K. Kundra, and B. C. Nakra "Prediction of dynamic characteristics using updated finite element models'' Department of Mechanical Engineering, Indian Institute of Technology, Hauz Khas, New Delhi, 110016, India.

[8]Peter Avitabile "Experimental Modal Analysis a Simple Non-Mathematical Presentation, University of Massachusetts Lowell, Massachusetts Sound and Vibration Presented at IMAC XXV February 19-22,2001

Future Directions Of Membrane Oxygen Separation Technology

Reepen Shah[1],Hardik Gangadia[2],Hetal Deshmukh[3]
[1,2,3]*Asst. Prof., Mechanical Engineering Department, Silver Oak College of Engineering and Technology , Ahmedabad, Gujarat, India*
[1]ripen2011@yahoo.com
[2]hgangadia@yahoo.com
[3]hetal02me109@gmail.com

***Abstract*- During the past 20 years, sales of membrane gas separation equipment have grown to become a $150 million/year business. More than 90% of this business involves the separation of non condensable gases: nitrogen from air; carbon dioxide from methane; oxygen from the air. This Paper deals with how oxygen is separated from the atmospheric air, materials used for separation of the oxygen and the factors which affects the separation of oxygen from atmospheric air.**

***Keywords*- Oxygen Separation, PSA, membrane, permeators.**

I INTRODUCTION

In 1980, Permea launched its hydrogen-separating Prism membrane. This was the first large industrial application of gas separation membranes. Since then, membrane-based gas separation has grown into a $150 million/year business, and substantial growth in the near future is likely. In this review, current membrane gas separation applications are surveyed.

Unlike nitrogen production, the practicality of membrane-based oxygen production depends strongly on improvements in membrane performance. Various approaches to using membranes to separate oxygen from air have been investigated. All rely on selectively permeating oxygen and rejecting nitrogen. Because air already contains 80% nitrogen and because nitrogen remains on the residue side of the membrane, producing essentially pure nitrogen is comparatively easy. Producing oxygen is more difficult because some nitrogen always permeates with the oxygen, resulting in oxygen enriched air rather than pure oxygen. The process was developed to the early commercial stage in the 1980s using silicone rubber and ethyl cellulose membranes, but the performance of these membranes was not good enough to make the process competitive with other technologies.

II OPERATING PRINCIPAL OF OXYGEN SEPARATION

The process of separation of oxygen from the atmospheric air is known as pressure swing adsorption process. Pressure Swing Adsorption (PSA) is a technology used to separate some gas species from a mixture of gases under pressure according to the species' molecular characteristics and affinity for an adsorbent material. It operates at near-ambient temperatures and so differs from cryogenic distillation techniques of gas separation. Special adsorptive materials (e.g., zeolites) are used as a molecular sieve, preferentially adsorbing the target gas species at high pressure. The process then swings to low pressure to absorb the adsorbent material.

Pressure swing adsorption processes rely on the fact that under pressure, gases tend to be attracted to solid surfaces, or "adsorbed". The higher the pressure, the more gas is adsorbed; when the pressure is reduced, the gas is released, or desorbed. PSA processes can be used to separate gases in a mixture because different gases tend to be attracted to different solid surfaces more or less strongly. If a gas mixture such as air, for example, is passed under pressure through a vessel containing an adsorbent bed that attracts nitrogen more strongly than it does oxygen, part or all of the nitrogen will stay in the bed, and the gas coming out of the vessel will be enriched in oxygen. When the bed reaches the end of its capacity to absorb nitrogen, it can be regenerated by reducing the pressure, thereby releasing the adsorbed nitrogen. It is then ready for another cycle of producing oxygen enriched air.

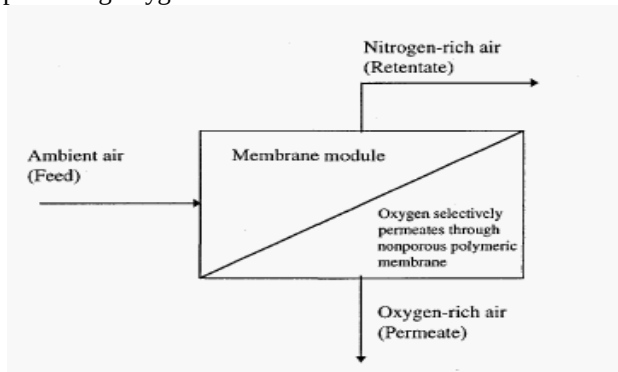

Fig.1 Basic Membrane process for air separation

A simplified flow schematic of a membrane separation process for producing oxygen-enriched air is shown in Fig. 1. Feed air containing 21% oxygen is passed across the surface of a membrane that preferentially permeates oxygen. In the schematic shown, the pressure differential across the membrane required to drive the process is maintained by drawing a vacuum on the permeate gas. The alternative is to compress the feed gas, but a few trial calculations show that this is never likely to be economical because of the quantity of electric power consumed. All of the feed air must be compressed, but only a small portion permeates the membrane as oxygen-enriched product. The power consumption of a vacuum pump on the permeate side of the membrane is one-half that of a feed compressor, because the only gas that needs to pass through the pump is the oxygen-enriched product. However, because the pressure difference across the membrane is less than 1 atm, vacuum operation requires a larger membrane area to produce the same flow of product gas. To make this operating mode economical, high-flux membranes and low-cost membrane modules are required.

2.1 Membrane Operating Mode

Air separation membrane units can be operated in one of three modes: vacuum, pressure, or mixed mode. In the vacuum mode, the feed air is pressurized to only slightly above atmospheric pressure (about 1 to 3 psig), and a vacuum is maintained on the permeate side of the membrane. The retentate is vented at atmospheric pressure.

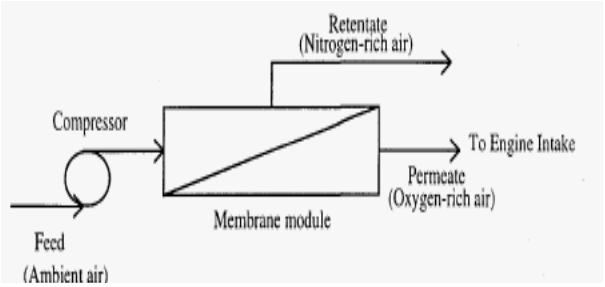

Fig.2 Membrane operating on pressure mode

The vacuum mode is typically more energy-efficient than the pressure mode, primarily because a vacuum is applied only on the permeate (product stream). However, because of the limited differential pressure, the vacuum mode requires a larger membrane area for a given flow rate than does the pressure mode. In the pressure mode, the feed air is typically pressurized (by an air compressor) to several atmospheres, while the permeate is maintained at about atmospheric pressure. Higher driving forces are obtained in this mode because the differential pressures are higher than those of the vacuum mode, resulting in reduced membrane area requirements. However, the pressure mode is more energy-intensive, because both permeate and retentate have to be compressed to higher pressures.

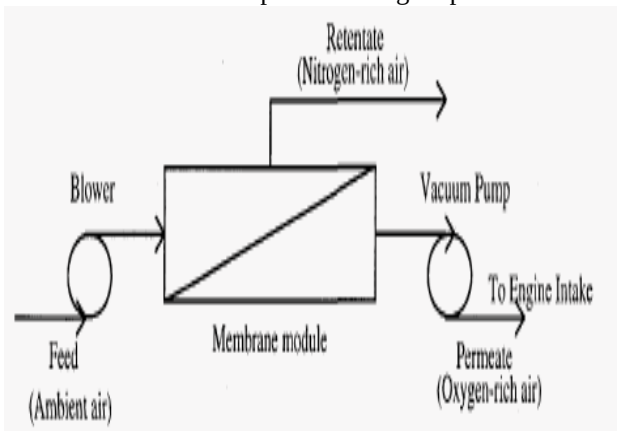

Fig.3 Membrane operating on vacuum mode

Finally, in the mixed mode, the feed air is pressurized, and a partial vacuum is maintained on the permeate side to increase both the compression ratio and differential pressure, and thus, the oxygen concentration.

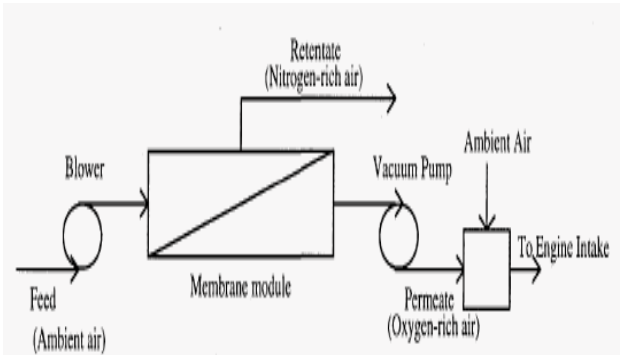

Fig.4 Membrane operating on Mixed mode

The oxygen-enriched air stream from the permeate is then mixed with an ambient air stream to obtain the desired air flow and oxygen concentration.

2.2 Factors Affecting Performance Of Air Separation Membrane

The performance of an air separator depends on the membrane's intrinsic properties and on several other parameters, such as membrane polymer structure, skin thickness, geometry of the fibers, fiber dimensions, flow pattern, feed direction, feed conditions, cartridge type, packaging density, and arrangement of separators. The selection of a membrane to achieve the desired oxygen-enriched air flow is evaluated in terms of the power required to maintain the differential pressure across the membrane and the amount of space it occupies. The

following sections briefly summarize the influence of certain key parameters on the performance of air separation membranes.

2.3 Polymer Structure

Polymeric solution-diffusion membranes for gas separation depend on the chemistry of the polymers and its influence on the rate at which gas molecules diffuse through the membrane. Rubbery and glassy polymers are the two classes of conventional materials used for gas separation. A rubbery polymer is an amorphous polymeric material that is above its softening or glass transition temperature under the conditions of use. These materials generally possess high permeability and low selectivity. A glassy polymer is an amorphous polymeric material that is below its softening or glass transition temperature under the conditions of use. Due to the more restricted segmental motions in glassy polymers, these materials offer enhanced selectivity with respect to rubbery polymers. As a result of growing interest in gas separation membranes, a host of new materials (grouped as polycarbonates and polymides) has been developed that are specifically designed to enhance gas permeability and selectivity.

2.4 Skin Thickness Of Membrane Coating:

For compact modules, the skin thickness of a membrane coating on a porous support (hollow fibers) is critical. The rate of gas transport across the membrane is inversely proportional to the skin thickness of the membrane (active) layer. When membrane material is coated over the porous support (hollow fibers), it is generally referred to as a composite membrane. The membrane must be mechanically strong to withstand pressure and temperature. For commercial membranes, skin thickness is typically on the order of 1000 to *2000* A, with 400 to 1000 A attainable in more finely tuned membranes. Apart from the skin thickness, the morphology of the membrane across the entire thickness also influences the ultimate performance of the membrane. Symmetric membranes (homogeneous) membranes have a uniform density across their thickness.

2.5 Geometry Of Membrane:

Two geometries are commonly used, flat films and hollow fibers. The membrane geometry influences the manner in which the membrane is packaged. Fig. 5 & 6 shows a schematic of flat-film and hollow-fiber membranes. Hollow fibers offer excellent packaging compared to flat films. In contrast to flat membranes, hollow fibers are self-supporting. The inside and outside of the fibers are in the range of 100-500 and 500-1000 micron respectively. The maximum external and internal pressures at which they can be operated are determined by the modules of the membrane material; the ratio of fiber OD and ID, and the detailed structure of the membrane.

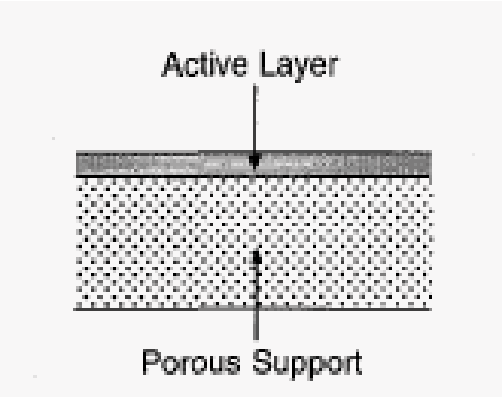

Fig.5 Flat film type membrane

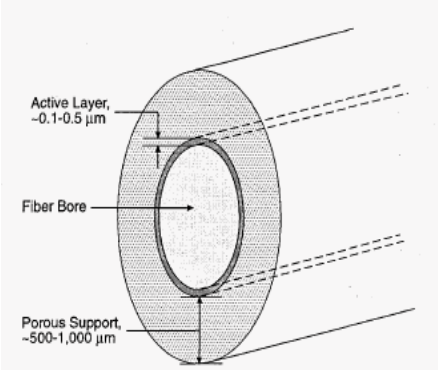

Fig.6 Hollow fiber type membrane

Regardless whether the membrane is fabricated as a flat sheet or a hollow fiber, it must be incorporated into a useful package that is readily usable. A compact membrane cartridge design should have a high packaging density, because the permeate gas flow per unit membrane area is inherently low. Flat sheet, spiral-wound, and hollow-fiber geometries are the three membrane cartridge options available; each has its advantages and limitations. Flat sheet modules resemble plate-and-frame press filter. Fig. 7 shows the elements of plate-and frame membrane module. The fabrication of such modules is relatively easy, but they give the lowest surface area per unit volume. Spiral wound cartridges consist of a number of leaves, each containing two flat sheets of membrane separated by porous support material, as shown schematically in Fig. 8. Spiral wound cartridges are reasonably compact, and system designs incorporating spirals require a simple pressure vessel. Such a cartridge provides area densities intermediate between the plate-and-frame and typical hollow fiber modules. However, gas by-pass around the cartridges due to “brine seal” misalignment or failure within the

pressure vessel is a potential concern that may reduce spiral wound cartridge productivity.

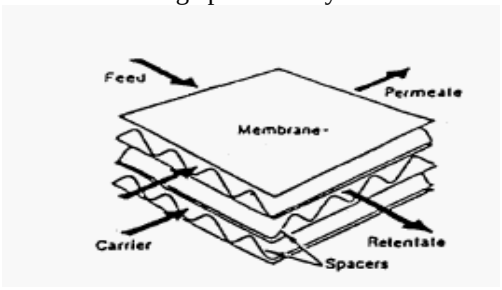

Fig.7 Plate and frame membrane module

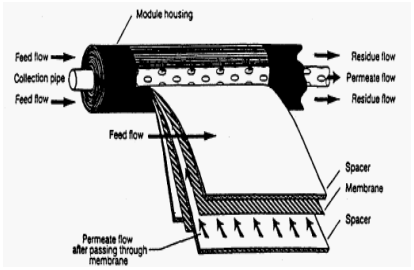

Fig.8 Spiral wound membrane module

In the case of hollow fibers, small hollow-fiber bundles were sealed with an adhesive into header plates at opposite ends of the module in such a way that a large number of fibers could be included. The packing density of hollow-fiber cartridge is the highest by far, compared to the other two cartridges, and this cartridge is simple to operate and maintain on clean gas stream. Typically, a hollow-fiber membrane module resembles a shell-and-tube geometry. Fig. 9 illustrates the elements of a typical hollow fiber membrane module.

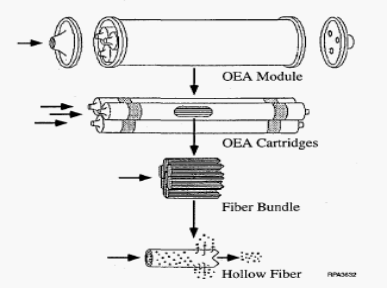

Fig.9 Hollow fiber membrane module

2.6 Flow Patterns:

The performance of the membrane separator is affected by the relative directions of feed and permeates flow in the vicinity of the active layer of the membrane and/or the relative flow directions of the bulk feed and permeate streams. The ideal flow patterns in a membrane are shown in Fig. 10. The feed and permeate streams may be directed co-currently or counter-currently to one another. Cross flow permeation, with the permeate stream perpendicular to the membrane, may also be practiced. For co- and counter-current permeation, the gas in contact with the downstream side of the membrane consists of gas that has just permeated through the membrane, plus the bulk permeates that is flowing past it. For cross flow permeation, on the other hand, the permeate gas that is in contact with, the active layer consists entirely of gas that has just passed through the membrane.

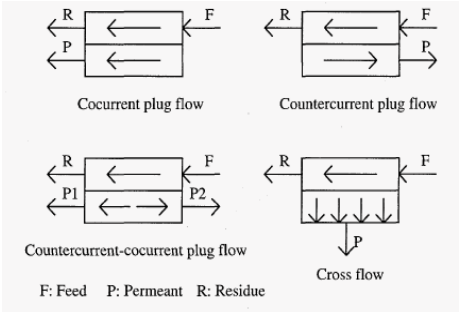

Fig.10 Ideal flow patterns in a membrane gas separation

2.7 Feed Direction:

In the shell-side feed permeators, the feed is brought in contact with the outer surface of the membrane fibers. Gas permeates into the fiber and then flows down the fiber bore, from which it passes through the tube sheet and out of the pressure vessel. In the tube-side feed permeators, the feed is delivered to the bore of the fibers. Two tube sheets are required, with feed gas being introduced through one tube sheet while non permeating gas exits from the other. The choice between shell-side and tube-side feed in hollow-fiber modules is generally made on the basis of the separation to be performed.

2.8 Feed Condition:

Raising the feed pressure results in a higher-purity permeate product when the separator is operated at the same fractional stage cut (recovery), although the extent of the increase diminishes at higher feed pressures. Undoubtedly, an increase in the feed pressure will lower the membrane area needed for a given fast gas recovery. Temperature is also an important variable that directly affects physical properties of the membrane, and hence its permeation and selectivity. The temperature limits for membranes are related to the glass transition temperature of the polymer. The permeability (product of the solubility and mobility coefficients) tends to be dominated by the diffusivity and increases with increasing temperature. On the other hand, the separation factor is moderated in its temperature-dependence because the temperature dependencies of the permeabilities of the various gases are rather similar. The addition of humidity to the feed air does

not appreciably affect the permeation because water vapor readily permeates the membrane.

2.9 Arrangements Of Separators:

The manner in which gas permeators are arranged with respect to one another is determined by both the module design and the process application. To increase the product recovery beyond what can be provided by the once-through (single-stage) systems, the membranes must be operated with recycling (multistage). Recycling of the permeate causes the feed composition to the membrane to increase, which results in a higher product purity at any given recovery. Recompression of recycled permeate adds both investment and operating cost to the membrane system; however, membranes can still be competitive in these cases.

III CONCLUSION

As discussed in this paper if atmospheric air is allowed to pass through the bed of selective materials (Activated carbon, Molecular Sieves, Zeolites) the separation of O_2 and N_2 takes place and as a result oxygen enrichment of atmospheric air is achieved. The many factors like Polymer Structure, geometry of membrane, flow patterns, feed direction, and feed condition affects the performance of air separation membranes. So while designing the membrane for air separation the above factors are required to be consider for optimum performance.

REFERENCES

[1]R.B.Poola, R. Sekar, D.N.Assanis, "Applications of oxygen enriched combustion to locomotive engine", Argon national laboratory.

[2]Anand, J.N., S.E. Bales, D.C. Feay, and T.O. Jeanes, 1989, "Tetrabromo Bisphenol Based Polycarbonate Membranes", U.S.Pattent.

[3]Gollan, A.Z., and M.H. Kleper, 1985, "Research into an Asymmetric Membrane Hollow Fiber Device for Oxygen-Enriched Air Production."

[4]Koros, W.J., and R.T. Chern, 1987, Handbook of Separation Process Technology, John Wiley and Sons.

[5]Ronald W. Rossoue, Handbook of Separation Process Technology.

[6]R.B.Poola, H.K.Ng, R. Sekar, "Utilizing Intake-Air Oxygen-Enrichment Technology to Reduce Cold-Phase Emissions."

Comparison Of Four Stroke & Six Stroke Engine According To P-V & Valve Timing Diagram

Mayur Surani[1],Reepen Shah[2],Jitendra Patel[3]
[1](Lecturer, Mechanical Engineering Department, Silver Oak College of Engineering and Technology, Ahmedabad, Gujarat, India)
[2](Asst. Prof., Mechanical Engineering Department, Silver Oak College of Engineering and Technology, Ahmedabad, Gujarat, India)
[3](3rd Semester, M. E.(Thermal), Gandhinagar Institute of Technology,Ahmedabad,Gujarat,India)
[1]Surani.mayur@gmail.com
[2]ripen2011@yahoo.com
[3]jitu_1639@yahoo.com

***Abstract*- Utilisation of exhaust in four stroke is a new concept of six stroke engine in which we are able to get semi power stroke by injection of water at the end of semi exhaust as we know steam can expands 1600 times volume so due to that expansion we may get semi power stroke by allowing half of the exhaust gases outside & remaining two compressed by energy stored in flywheel.**

***Keywords*- Six stroke cycle, P-V Diagram, Valve Timing Diagram, Water Injection**.

I INTRODUCTION

Under the hood of almost all modern automobiles there sits a four-stroke internal combustion engine (ICE). Though the efficiency of the design has been improved upon significantly in the intervening years, the basic concept is the same today as that used by the first practical four-stroke engine built in the 1870s. During every cycle in a typical car engine, each piston moves up and down twice in the chamber, resulting in four total strokes, one of which is the power stroke that provides the torque to move the vehicle. But the automotive industry may soon be revolutionized by a new six-stroke design which adds a second power stroke, resulting in a much more efficient and less polluting alternative.

The six-stroke I. C. Engine described in this graph is designed to overcome many of the limitations inherent in the Otto cycle and bring the engine's operating cycle closer to Changed efficiency conditions. The preferred fuel for the concept engine is Gasoline and Water because of its latent heat and its ability to cool
the fuel/air charge during the combustion process.

1.1 Disadvantages Of Four Stroke Cycle

The disadvantage of the four-stroke cycle is that only half as many power strokes are 2 completed per revolution of the crankshaft as in the two-stroke cycle and only half as much power would be expected from an engine of given size at a given operating speed.

The four-stroke cycle, however, provides more positive scavenging and charging of the cylinders with less loss of fresh charge to the exhaust than the two-stroke cycle. Modern Otto cycle engines, such as the standard gasoline engine, deviate from the Beau de Rochas principles in many respects, based in large part upon practical considerations related to engine materials and the low-octane fuel used by the engine.

1.2 Crower Six-Stroke Engine

In a six-stroke engine developed in the U.S. by Bruce Crower, fresh water is injected into the cylinder after the exhaust stroke, and is quickly turned to superheated steam, which causes the water to expand to 1600 times its volume and forces the piston down for an additional stroke.[9] This design also claims to reduce fuel consumption by 40%. Maximum efficiency would theoretically be obtained by applying the design to a non-turbocharged diesel engine, where the high compression ratio would allow greater expansion of the steam.

The Crower six-stroke engine was invented in 2004 by 75 year old American inventor Bruce Crower who has applied for a patent on a design involving fresh water injection into the cylinders. As of May 2008, no patent has been awarded. Leonard Dyer invented the first six-stroke internal combustion water injection engine in 1915, which is very similar to Crower's design. Crower's six-stroke engine features:

- No cooling system required
- Improves a typical engine’s fuel consumption
- Requires a supply of distilled water to act as the medium for the second power stroke

1.3 Working Of Six Stroke Cycle

1) The fuel/air valves open as the piston moves down, which draws air and fuel into the chamber.

2) The valves close as the piston moves back up, putting the air/fuel mixture under pressure.

3) The mixture is then ignited, causing a small explosion which forces the piston back down, which turns the crank and provides the torque; and finally.

4) The exhaust valves open as the piston moves back up once again, pushing the byproducts of the fuel explosion out of the chamber. This leaves the piston back in its starting position, ready for another cycle. This process is repeated thousands of times per minute.

We all know, the combustion engine does not really convert the potential energy in fuel to kinetic energy to move the car efficiently. We lose a lot of that power – roughly 76% – in the form of heat. BMW has tried to salvage some of this lost energy with Turbo-charger system.

In a six stroke engine, two extra strokes are added to the customary internal combustion engine four stroke Otto cycle, which makes a six stroke engine. A third down-stroke is a "steam stroke" and a third up-stroke exhausts the expanded steam while venting heat from the engine.

The engine cold starts on the Otto cycle, coasting through the fifth and sixth strokes for a short period. After the combustion chamber temperature reaches approximately 400 degrees Fahrenheit (200 °C), a mechanical operation phases in the fifth and sixth strokes. Just before the fifth stroke, water is injected[1] directly into the hot combustion chamber via the engine's fuel injector pump, creating steam and another power stroke. The phase change from liquid to steam removes the excess heat of the combustion stroke forcing the piston down (a second power stroke). As a substantial portion of engine heat now leaves the cylinder in the form of steam, no cooling system radiator is required. A proportion of the energy that is dissipated in conventional arrangements by the radiator in a water-based cooling system has been converted into additional power strokes.

II COMPARISION FOUR STROKE WITH SIX STROKE

2.1 P-V DIAGRAM

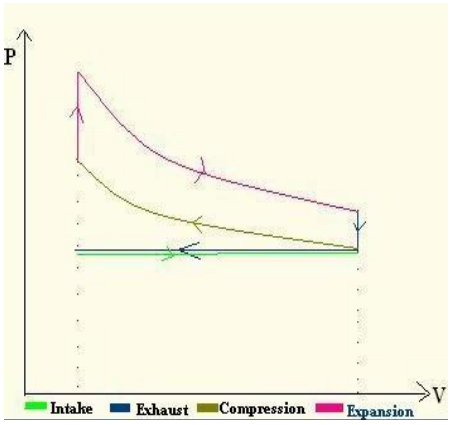

Fig.1 P-V Diagram 4 Stroke Petrol Engine

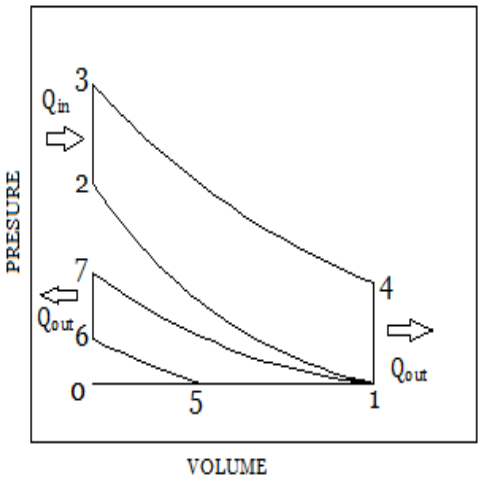

Fig.2 P-V Diagram 6 Stroke Petrol Engine

P-V Diagram 4 Stroke Processes	P-V Diagram 6 Stroke Processes
Process 0-1 – Intake	Process 0-1 – Intake
Process 1-2 – Compression	Process 1-2 - Compression-1
Process 2-3 – Combustion	Process 2-3 – Combustion
Process 3-4 - Expansion	Process 3-4 - Expansion-1
Process 4-1 Exhaust	Process 4-1 - Blow Down
-	Process 1-5 - Exhaust-1
-	Process 5-6 – Compression-2
-	Process 6-7 – Water Injection
-	Process 7-1 – Expansion-2
-	Process 1-0 – Exhaust-2

2.2 Valve Timing Diagram [2]

Four Stroke Petrol Engine	Six Stroke Petrol Engine
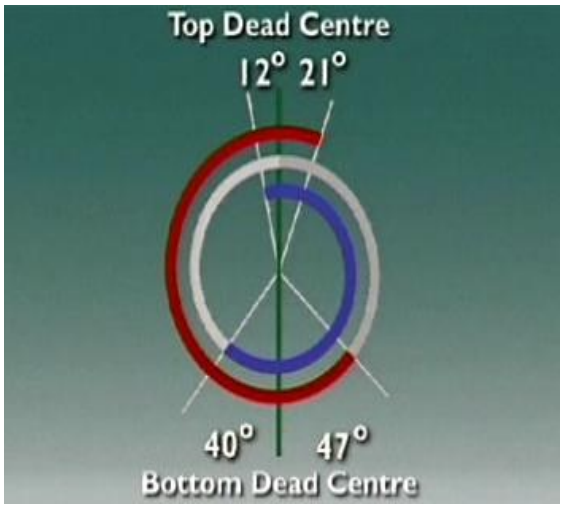	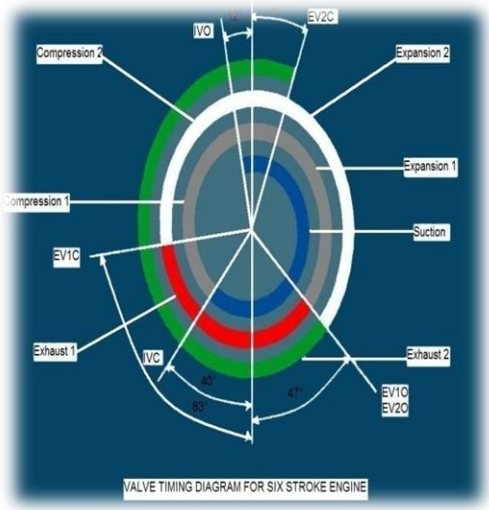
Opening and closing of Inlet Valve: The inlet valve is made to open 10degree to 30degree before the piston reaches the Top Dead Center (TDC) during Suction Stroke and is allowed to close only after 30degree to 40degree after the piston reaches and leaves the BDC in the beginning of compression stroke. **Opening and closing of Exhaust Valve:** The exhaust valve is made to open 30degree to 60degree before the TDC in the exhaust stroke and allowed to close only after 80 to 10 in0 the beginning of the suction stroke.	The valve timing for a six stroke engine is initially the same as that of a four stroke engine, in which various optimizations are done in the timing of the opening and closing of the valves in order to gain higher efficiency. The various movements of inlet and outlet valves are as follows: 1. Inlet valve opens at 12˚ before TDC. 2. Inlet valve closes at 40˚ after BDC. 3. Exhaust valve opens at 47˚ before BDC during EXHAUST-1. 4. Exhaust valve closes at decided angle (taken as 83˚ in the valve timing diagram below) after, BDC after EXHAUST-1. 5. Exhaust valve opens at 47˚ before BDC during EXHAUST-2. 6. Exhaust valve closes at 21˚ after BDC, after EXHAUST-2

2.3 Positive Aspect

Crower claims a 40% reduction in fuel consumption and reduced exhaust emissions per a given power range.

The principal advantage of the six-stroke design is its ability to extract work from heat that is ordinarily lost through the cooling system of a conventional engine. Since the steam strokes have the side-effect of cooling the engine internally, this will allow the use of much higher compression ratios, allowing the full potential of a fuel to be extracted. This internal cooling allows high compression ratios once usable for only short term applications (such as race engines) to be used in regular, long-running time scenarios without environmentally harmful anti-knock chemicals. Ultra-lean air/fuel mixtures, desirable for low emissions and high efficiency, may be used since excess heat, undesirable in other engine architectures, can likewise be harnessed in six-stroke applications[3]. The weight and power loss of most conventional cooling system parts, such as the fan, radiator, and coolant pump, can be eliminated. On a large diesel truck, these parts make up approximately a quarter of the engine's weight. At least a portion of this advantage is lost if water is recovered from the exhaust through a condenser.

The mechanical modifications needed to "six-stroke" a small air-cooled industrial diesel already being manufactured are far less complicated than any hybrid system, Many maintenance features of this engine would be parallel or identical to the knowledge base of mechanics well-versed with gasoline, diesel, and racing engines.

Physical engine size reduction (per a designated power rating) is possible as one third of the engine strokes produce power (in the Crower six-stroke), instead of one quarter (in the Otto cycle). This, and the extra power stroke being provided by using water instead of fuel, means there is a significant improvement to the fuel efficiency and pollution within a given power

range, and this is in a field where small improvements create great interest.

The higher percentage of power strokes may allow lower working speeds, with higher torque output at lower and broader rpm ranges. Lower working speed might allow designs with greater crankshaft diameter, for engine dimensions with inherently more torque potential.

As a high pressure steam engine that does not need a certified pressure boiler, the related hardware complexities, dangers, and weight penalties and certification requirements are removed.

III CONCLUSION

On the basis of the theoretical and analytical aspects of six stroke engine, it definitely looks as a bright invention which has the potential to revolutionize the world of engines and can be the next big thing in the field of IC engines in the near future. Though the exact changes in the fuel economy of the engine is yet to be practically observed, it certainly looks evident from the theoretical point of view that the engine is going to be much improved as far are its fuel economy is concerned and this forms the basis of the anticipation my team has for the six stroke engine. Also the fact that six stroke engine that we are up for, doesn't need much manufacturing changes and can be easily be adopted by the manufacturers of IC engines without any hassle. The fact that it can be easily adopted by both gasoline and diesel engines makes six stroke engine even more interesting. Thus we are very keenly looking forward to practically prove the finding, which is certainly going to be our next step towards making our project successful.

REFERENCES

[1] Conklina J. C. and Szybist J. P., "A Highly Efficient Six-Stroke Internal Combustion Engine Cycle with Water Injection for In-Cylinder Exhaust Heat Recovery", Energy, Volume 35, Issue 4, pp. 1658-1664 , 2010.

[2] Nwafor OMI. Effect of advanced injection timing on the performance of rapeseed oil in diesel engines. International Journal of Renewable Energy2000;21:433–44

[3] Robin Kumar, Govind Pal Singh, Amarnath Pandey, Rajeev Ranjan, Vikas Kumar, Innovation In Marine Diesel Engine Scavenging With A New Approach, Marine engineers review, Volume-5, Issue 4, pp. 13-20, 2011.

[4] George Marchetti and Gilles Saint-Hilaire, A Six-Stroke, High-Efficiency Quasiturbine Concept Engine, www.quasiturbine.com/QTMarchettiSthSixStroke0509.pdf, September 2005

[5] Andrew De Jong, team 6 stroke, https://knightvision.calvin.edu.

[6]High speed internal combustion engines by John B. Heywood.

Adsorption Air Conditioners Driven By Exhaust Gases

Jitendra Patel[1],Reepen Shah[2],Mayur Surani[3]
[1](3rd Semester, M. E.(Thermal), Gandhinagar Institute of Technology,Ahmedabad, Gujarat, India)
[2](Asst. Prof., Mechanical Engineering Department, Silver Oak College of Engineering and Technology, Ahmedabad Gujarat ,India)
[3](Lecturer., Mechanical Engineering Department, Silver Oak College of Engineering and Technology, Ahmedabad, Gujarat, India)
[1]jitu_1639@yahoo.com
[2]ripen2011@yahoo.com
[3]Surani.mayur@gmail.com

***Abstract*- This paper presents the achievements in solid sorption refrigeration prototypes obtained since the interest in sorption systems was renewed at the end of the 1970s. The applications included are ice making and air conditioning. The latter includes not only cooling and heating, but also dehumidification by desiccant systems. The prototypes presented were designed to use waste heat or solar energy as the main heat sources. The waste heat could be from diesel engines or from power plants, in combined cooling, heating and power systems (CCHP). The current technology of adsorption solar powered icemakers allows a daily ice production of between 4 and 7 kg per m2 of solar collector with a solar COP between 0.10 and 0.15. The silica gel-water chillers studied can be powered by hot water warmer than 55 °C. The COP is usually around 0.2 to 0.6, and in some commercially produced machines, the COP can be up to 0.7. The utilization of such chillers in CCHP systems, hospitals, buildings and grain depots are discussed. Despite their advantages, solid sorption systems still present some drawbacks such as low specific cooling power and COP. Thus, some techniques to overcome these problems are also contemplated, together with the perspectives for their broad commercialization.**

***Keywords*- CCHP, Adsorber, Regenerator, Waste Heat, Air conditioning.**

I INTRODUCTION

The interest in adsorption systems started to increase, firstly due to the oil crisis in the 1970s that lead to a concern about the energy shortage, and then later, in the 1990s, because of ecological problems related to the use of CFCs and HCFCs as refrigerants. Such refrigerants, when released into the atmosphere, deplete the ozone layer and contribute to the greenhouse effect. Furthermore, with the increase of the energy consumption worldwide, it is becoming even more urgent to find ways of using the energy resources as efficiently as possible. Thus, machines that can recover waste heat at low temperature levels, such as adsorption machines, can be an interesting alternative for a wiser energy management.

Zhang [1] studied an adsorption air conditioning system that could have the sorption beds regenerated by the exhaust gases of a bus. The adsorber consists of two concentric pipes, and the exhaust gases or the cooling air flowed through the inner pipe, to release or remove heat from the adsorbent, respectively. The adsorbent (zeolite) was placed between the inner and the outer pipe. Fins were attached to the inner pipe to increase the heat transfer between the fluids and the adsorbent, and water was used as refrigerant

The COP found was 0.38 and the SCP was 25.7 Wkg-1. The author also calculated the coefficient of waste heat cooling (WCOP), which takes into account the potential waste heat that can be recovered to produce the cooling effect, without the gas reaches the dew point. The value of WCOP found for this system was 0.31. This author suggested that the WCOP is more suitable than the COP to identify which cooling capacity could be produced from the exhaust gases of diesel engines, because in a real application, it is desirable that the gas never reaches the dew point to avoid corrosion of the adsorber.

Lu et al. [2] developed an air conditioner with the pair zeolite-water that could be powered by the exhaust gases of a locomotive. This system, which scheme is shown in Fig. 21, was based on a laboratory prototype developed by Jiangzhou et al. [3]. It was designed to refrigerate the driver's cabin of a locomotive that ran in the Zhejiang province, East China.

The cooling power of such a system under typical running conditions ranged from 3 to 5 kW, with a COP of 0.21. The temperature inside the cabin was between 4 and 6 °C lower than the ambient temperature, while this same cabin, without refrigeration usually had a temperature of 2 to 5 °C higher than the ambient temperature.

II APPLICATION

Air conditioning on vehicles could be another reasonable application for adsorption systems powered by exhaust gases. The vehicles more suitable for this kind of air conditioner are buses and locomotives, as adsorption systems usually still have large volume and mass.

III USE OF WASTE HEAT IN REGENERATOR

The simple vapour absorption system consist of an absorber, a pump, a generator and a pressure reducing vavle to replace the compressor of vapour compression system. The other components of the system are condenser, receiver, expansion valve and evaporator as in the vapour compression system.

In this system, the low pressure ammonia vapour leaving the evaporator, enter the absorber where it is absorbed by the cold water in the absorber. The water is a absorbent, than this strong solution goes to generator. The heat is supply in generator by external sources. In generator ammonia and water is separated and weak solution return to absorber ant ammonia goes to condenser.

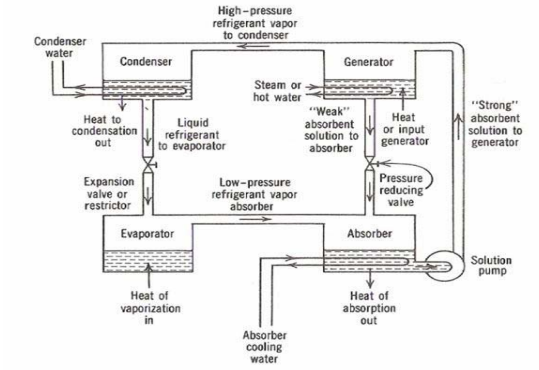

Fig.1 Waste heat usage in regenerator

Lu et al. developed an air conditioner with the pair zeolite-water that could be powered by the exhaust gases of a locomotive. This system, which scheme is shown in Fig. 1, was based on a laboratory prototype developed by Jiangzhou et al. [3]. It was designed to refrigerate the driver's cabin of a locomotive that ran in the Zhejiang province, East China**.**

The cooling power of such a system under typical running conditions ranged from 3 to 5 kW, with a COP of 0.21. The temperature inside the cabin was between 4 and 6 °C lower than the ambient temperature, while this same cabin, without refrigeration usually had a temperature of 2 to 5 °C higher than the ambient temperature.

Zhang [1], with respect to the cooling of the adsorbent in the adsorption phase.In the experiments with this machine, the temperature of the adsorbent bed at the end of the adsorption phase was close to 90 °C, which greatly reduced the cooling performance. The authors remarked that the velocity of the locomotive and the rotating speed of the engine have significant influence on the cooling and heating power, respectively, of the air conditioner.This system is feasible and practical to be applied in a locomotive except when it pulls passenger cars, because in this condition, the train runs slowly and stops at every railway station. The cost of such a system is expected to be about US$5,000.

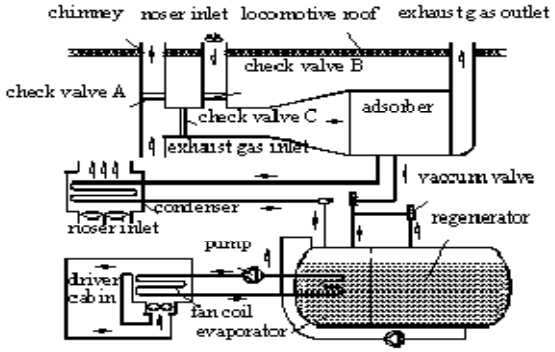

Fig.2 Regenerator laboratory prototype

In this type of system heat is provided to regenerator by exhaust gases.

IV HEAT PIPES

The high initial costs of the machines and the low heat transfer properties of the adsorbers are among the limitations for the commercial application of adsorption systems. The use of heat pipes could help in the reduction of these problems, not only due to the high heat flux density provided by these devices, but also due to the lack of moving parts to drive the heat transfer medium, which makes the whole system cheaper and more reliable.

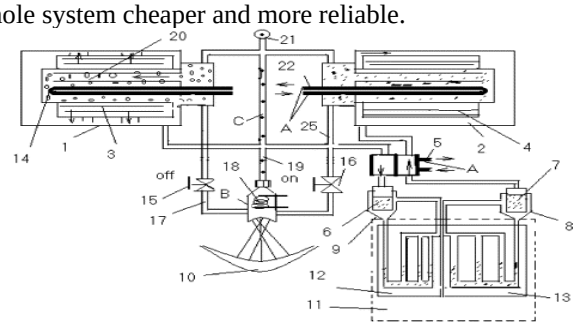

Fig.3 Heat pipes mechanism for exhaust gases

Meunier [4] mentioned a study carried out at LIMSI where extremely high heat transfer coefficients of about 10 kWm-2 were obtained with the utilization of heat pipes in adsorption systems.

Critoph [5] applied a heat pipe to heat and to cool the adsorber of an adsorption system. The author concluded that different fluids should be used for cooling and heating purposes. Fluids with different physical properties would avoid sub-atmospheric and very high working pressure, which is desirable because it eliminates both the occurrence of possible inward air leaks and the utilization of thick material to enclose the working fluid

Vasiliev et al. [6] designed an adsorption system that could be powered by solar energy or electricity. Heat pipes were used in the heat transfer fluid and refrigerant circuits.

The heat sources supplied the necessary energy to evaporate the working fluid inside one of the heat pipe evaporators (16 in Fig. 3). When this fluid condensed, it released heat to regenerate the adsorbents (2). The two phase heat transfer device of this system was constructed as a vapour dynamic thermosyphon, which had one small boiler evaporator (16), two elongated cylindrical condensers inside the adsorber (9), a vapour chamber (16) with two flexible pipes for liquid flow (11), and one pipe for vapour flow (13). There were also two valves (10) on the pipes for liquid flow that were used to regulate the feeding of water into the boiler.

A loop heat pipe was used to connect the refrigerant evaporator of the adsorption system (4 in Fig. 26) to the cold box. The condenser of the heat pipe (5) was placed on the outer surface of the refrigerant evaporator. The evaporation part of the multi-bent heat pipe was inserted along the walls of the refrigerator. These two heat pipes arcs were used as a second ammonia circuit, thermally connected with the first ammonia circuit (evaporators 4). When the temperature of the evaporators decreased and became lower than the temperature of the air inside the refrigerator, the ammonia inside the heat pipe evaporated to condensate on the outer surface of the evaporator. The heat transfer between the air inside the refrigerator and the cold heat pipe panel was performed by natural convection, and this panel could provide 300 W of cooling**.**

V PERFORMANCE OF ADSORPTION SYSTEMS FOR AIR CONDITIONING

Application	Heat source temperature or insolation	Working Pair	COP	SCP or ice production	Year	Ref.
Air conditioning	232 °C	AC-NH_3	0.42-1.19	[6]NA	1996	102
Air conditioning	204 °C	Zeolite-Water	0.6-1.6	36-144 W kg^{-1}	1988	101
Air conditioning	230 °C	Zeolite-Water	0.41	97 W kg^{-1}	1999	31
Air conditioning	310 °C	Zeolite-Water	0.38	25.7 W kg^{-1}	2000	80
Air conditioning	100 °C	AC-NH_3	0.2	600 W kg^{-1}	2003	87
Air conditioning	230 – 300 °C	Zeolite-Water	0.20 - 0.21	21.4 – 30 W kg^{-1}	2004	85

VI CONCLUSIONS

Since the interest in adsorption systems was renewed in the last 20 years, the COP and the SCP of these systems greatly increased due to the work of several research groups. The results should not be compared to one another, as they were obtained under different working conditions, but they should be used as a reference of what can be expected from these systems.

After several projects aimed to increase the performance of the adsorption chillers with the pair silica gel-water, these chillers can be currently found on the market and they are already under operation as part of the air conditioning systems located in buildings or in a chinese grain depot.As the adsorptive beds of the chillers can be regenerated by low-grade temperatures, waste heat or solar energy can be used as heat source. These chillers can also be employed in CCHP systems as demonstrated by the application in a hospital situated in Germany, and by recent studies in the Shanghai Jiao Tong University. The overall thermal and electrical efficiency in these systems can be above 70%. When applied to commercial buildings, a CCHP with rated electricity power of 12 kW, rated cooling power of 10 kW and rated heating power of 28 kW would have a payback period of between 2 and 3.2 years if the price of thenatural gas ranged from US$ 0.19 to 0.23 .

The cost of adsorption chillers, that nowadays is about US$ 7,000 for a 10 kW-unit, could be reduced by mass production and by the use of technologies that could reduce or simplify their components. Heat pipes are among the technologies suitable to accomplish such a goal, as demonstrated with some experiments performed at the SJTU.

REFERENCES

[1] L. Z. Zhang, 2000, Design and testing of an automobile waste heat adsorption cooling system. Appl. Thermal Engng. 20; 103-114.

[2] Y. Z. Lu, R. Z. Wang, S. Jianzhou, Y. X. Xu, J. Y. Wu, 2004, Practical experiments on an adsorption air conditioner powered by exhausted heat from a diesel locomotive. Appl. Thermal Engng. 24; 1051-1059.

[3] S. Jiangzhou, R. Z. Wang, Y. Z. Lu, Y. X. Xu, J. Y. Wu, 2002, Experimental investigations on adsorption air-conditioner used in internal-combustion locomotive driver-cabin. Appl. Thermal Engng. 22; 1153-1162.

[4] F. Meunier, 1998, Solid sorption heat powered cycles for cooling and heat pumping applications. Appl. Thermal Engng. 18; 715-729.

[5]R. E. Critoph,2000, The use of thermosyphon heat pipes to improve the performance of a carbon–ammonia adsorption refrigerator. Proc. of the IV

Minsk Int. Seminar - Heat Pipes, Heat Pumps, Refrigerators; Belarus.

[6] L. L. Vasiliev, D. A. Mishkinis, A. A. Antukh, L. L. Vasiliev Jr., 1999, A solar and electrical solid sorption refrigerator. Int. J. Therm. Sci. 38, 220-227.

[7] Z. Z. Xia, R. Z. Wang, J. Y. Wu, D. C. Wang, 2003, New type of effective adsorption chiller adopt separate heat pipe (in Chinese). Chinese Patent 200410025398.0.

[8] Z. Z. Xia, R. Z. Wang, J. Y. Wu, L. W. Wang , 2004,Compound alternate heat pipe reactor powered by waste heat (in Chinese). Chinese Patent 200410018291.3.

[9]P. Bou, J. J. Guilleminot, M. Pons,1996 Composite actif à structure feuilletée comprenant un agent actif sous forme de granules. Elf Aquitaine Patent, 9612762

Multicasting in MANET using Mesh Based Protocol

Vikas N. Tulshyan
Department of Computer Engineering, Silver Oak College of Engineering & Technology, Ahmedabad
vikasntulshyan@gmail.com

***Abstract*- A mobile ad-hoc network is composed of mobile nodes. MANET is not having any infrastructure. Over radio links mobile nodes self-organize to form a network. There are many applications like military battlefields, rescue sites where rapid deployment is necessary and even wired network is not available. The efficiency of the wireless link can be improved by multicasting. There is a comparative study of various multicasting routing protocols. On Demand Multicast Routing Protocol (ODMRP) is well suited for near Real Time Systems. Concept of Network Coding is introduced in existing ODMRP multicast protocol. Three performance metrics are Packet Delivery Ratio, Throughput and Delay are measured. ODMRP with Network Coding improves Packet Delivery Ratio, Throughput and Delay.**

***Keywords*- Mobile ad-hoc network (MANET), Multicast Routing Protocol, Network Coding**

I INTRODUCTION

Multicasting means transmission of packets to a hosts which are having single destination address. In multicasting there is group oriented computing, where the membership of a host group is typically dynamic that is, hosts may join and leave groups at any time. Restriction is not there about the location as well as members in the host group.

II RELATED WORK

On-Demand Multicast Routing Protocol (ODMRP) [2] is a reactive mesh based multicast routing protocol. ODMRP is not only a multicast routing protocol, but also provides unicast routing capability. The source establishes and maintains group membership and multicast mesh on demand if it needs to send data packets to the multicast group, which is somewhat similar to MAODV. A set of nodes, which is called forwarding group, participate in forwarding data packets among group members. All the states in ODMRP are soft states, which are refreshed by the control messages mentioned above or data packets, which achieves higher robustness.

ODMRP uses a forwarding group concept for multicast packet transmission, in which each multicast group G is associated with a forwarding group (FG). Nodes in FG are in charge of forwarding multicast packets of group G. In a multicast group of ODMRP, the source manages the group membership, establishes and updates the multicast routes on demand. Like reactive unicast routing protocols, ODMPR comprises two main phases: the request phase and the reply phase.

A multicast source floods a Join Request packet to the network, when it has no routing and group membership information but has a packet to send.. Join Request packets are member-advertising packets with piggybacked data payload.. A JOIN Request packet reaches a multicast receiver, the receiver refreshes or creates an entry for the source in Member Table and broadcasts JOIN TABLE packets. When a node receives a JOIN TABLE packet, it checks each entry of the table to find out if there is an entry in the table whose next node ID field matches its ID.

If there is a match, the node recognizes that it is on the path to the source, thus it is part of the forwarding group. Consequently, each member of a forwarding group propagates the JOIN TABLE packets until the multicast source is reached via the shortest path. This process constructs (or updates) the routes from sources to receivers and builds a mesh of nodes, the forwarding group.

Network coding is a method of optimizing the ow of digital data in a network by transmitting digital evidence about messages. The "digital ev-idence" is, itself, a composite of two or more messages. When the bits of digital evidence arrive at the destination, the transmitted message is deduced rather than directly reassembled.

The core concept of Network Coding is to allow encoding of data packets at intermediate nodes and a receiver decodes original data when it gets enough encoded packets.Ahlswede et al.[4] who showed that the multicast capacity can be achieved by Network Coding mixing information from dif-ferent flows. In Network coding, instead of forwarding packets as it is, nodes may recombine two or more input packets into one or more output packets.

In [3], Christina Fragouli. proved that linear coding obtains the multicast capacity bound,in addition, Ho et al. showed that random coefficients over a sufficiently large finite field can be adopted to reach the capacity bound. The random coefficients

are determined in a distributed manner by random linear coding.

We assume that each packet contains L bits. If packets to be combined are not of the same size, smaller packets are padded with trailing zeros. S consecutive bits of a packet can be interpreted as a symbol over the field F2s . i.e., each packet consists of a vector of L/s symbols. Outgoing packet at each node is linear combination of incoming packets or generated packets at that node where addition and multiplication operations are performed over the field F2s . The encoded packet also contains L bits. So an encoded packet contains information about all original packets and multiple such packets can be generated. In e_ect, information of an original packet is spread into number of encoded packets.

.

III PROPOSED ALGORITHM

In the existing protocol, ODMRP, after route construct process between source and destination, multicast source start to transmit packets. The route from source to destination may fail due to any reason. So the routing process should start again to find a new route as packets are lost. This procedure causes PDR reduction. Now in order to increase the PDR, in the dynamic network we introduce the concept of network coding as shown in Fig. 1.

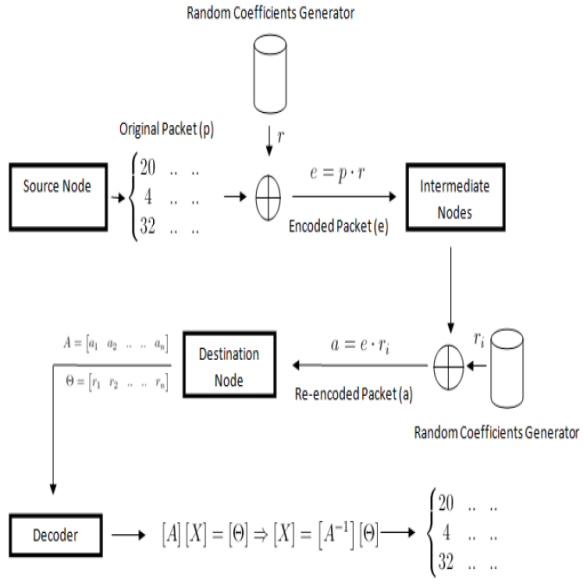

Fig.1 Block Diagram showing how the packets are encoded and decoded

The route discovery for the first time happens in a regular way. Once the route discovery happens, the source starts to transmit packet using network coding mechanism. The source encodes the packets by taking the dot product of randomly generated co-efficient and first byte of each packet.

This encoded packet is then forwarded to intermediate node selected using ODMRP. The intermediate node upon receiving the encoded packet, re-encodes it with its own random coefficient, and forwards to its intermediate neighbors, not only to those who are in the shortest path, but to all. A re-encoded packet is generated of the generation which has the maximum number of encoded packets to be sent. The re-encoded packet is the mixture of all the independent packets stored at the node for the generation.

Hence using this concept, even in the dynamic nature of the network, the destination node can receive encoded packets from one or other nodes. This increases the PDR, as the packets sent by the source are always present in the network. Also the packets are not redundant; hence the packets don't get dropped also. The destination node upon receiving m linearly independent encoded vectors, decodes the system using the following mechanism.

Let the received the set be $(r^1, a^1),\ldots\ldots,(r^n, a^n)$.In order to retrieve the original packets , it needs to solve the system $X = A^{-1} \bullet \Theta$. In this linear sytem there are m equations and n unknowns. Number of packets received should be atleast as large as number of original packets.

IV SIMULATION RESULTS AND DISCUSSION

We have simulated the protocol in NS2 Simulator. A network contains 100 nodes which move according to Random Way Point model. Simulation duration is 100 sec. The mobility model uses a random waypoint model with 50 nodes. Here each node starts its journey from a random location to a random destination with a randomly chosen speed from 20mps to 80 mps. It is Observed that, compare to traffic speed inside a city ad hoc network has fairly high speed. Once the destination is reached, another random destination is targeted after a pause. Node bounces back and continue to move when it reaches the simulation terrain boundary.

When we have simulated the existing ODMRP protocol and compared it with the concept of Network Coding the results are as shown in the graph.

From the results shown in Fig. 2, it is clear that as mobility increases, the Packet delivery ratio improves. The performance of algorithm with Network coding is approximately 13 to 16% better than existing ODMRP Protocol at a mobile speed in the range of 70 to 100 m/s.

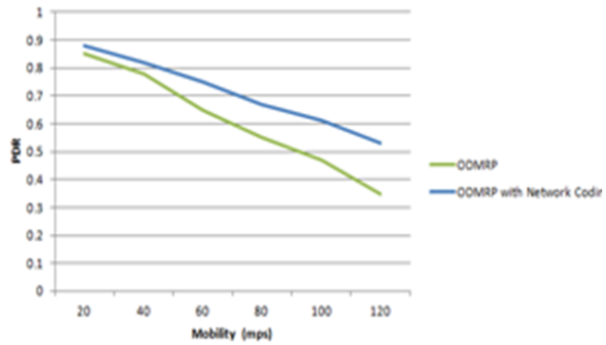

Fig.2 Graph Showing Result of PDR vs. Mobility

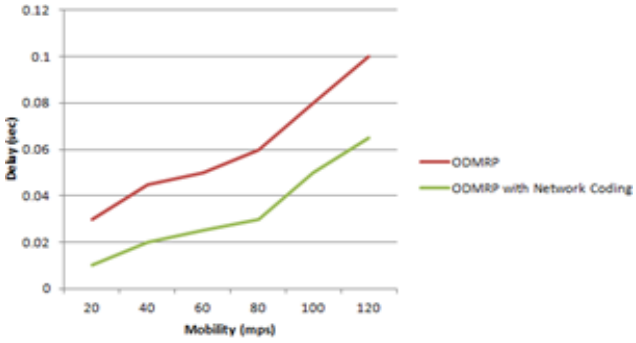

Fig.3 Graph Showing Result of Delay vs. Mobility

From the results shown in Fig. 3, when delay is measured against Mobility with existing ODMRP Protocol, there is 3ms to 10ms delay in the mobility of 20 to 80mps.When same is simulated with network Coding concept it is improved.

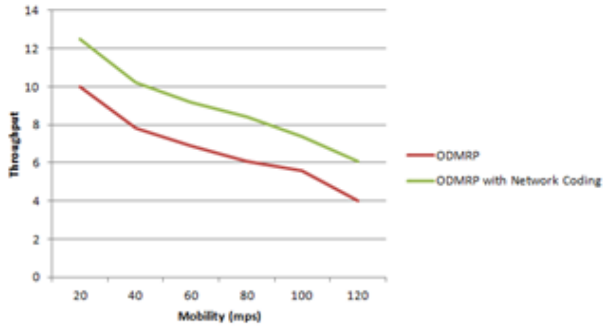

Fig.4 Graph Showing Result of Throughput vs. Mobility

As shown in graph throughput decreases with increase in mobility. As mobility increases the throughput goes from 10kb/s to 5 kb/s. When Network coding is implemented then it improves.

V FUTURE WORK

Optimize the solution, by allowing the network coding concept for forwarding packets on selected routes, rather than ooding the network. Also try to prevent excess amount of route discovery for dynamic network changes.

VI CONCLUSION

ODMRP is mesh based protocol .In this packets are forwarded by creating mesh from source to destination. Three Performance Metrics Packet Delivery Ratio, Throughput and Delay were measured. By using Network Coding concept in existing ODMRP protocol improves all the three metrics

REFERENCES

[1] S. Chachulski, M. Jennings, S. Katti and D. Katabi, Trading Structure for Randomness in Wireless Opportunistic Routing, SIGCOMM'07, Kyoto, Japan, pp. 169-180

[2] Christina Fragouli, Jean-Yves Le Boudec, and Jorg Widmer. Network coding: An instant primer. In ACM SIGCOMM Computer Communication Review, January 2006.

[3] R. Ahlswede, N. Cai, S. Li, and R. Yeung, Network information flow IEEE Transactions on Information Theory, 46:1204-1216, 2000.

[4] D. S. Lun, M. Medard, and R. Koetter, E_cient operation of wireless packet networks using network coding. In IWCT, 2005.

[5] Christina Fragouli, Jorg Widmer, and Jean-Yves Le Boudec. On the bene_ts of network coding for wireless applications.

[6] Shuo-Yen Robert Li, Raymond W. Yeung, and Ning Cai. Linear net-work coding. In IEEE Transactions on Information Theory, vol. 49, pp. 371- 381, February 2003.

[7] Kevin Fall and Kannan Varadhan,editors. ns Notes and Documen-tation. The VINT Project,UC Berkeley,LBL,USC/ISI, and XEROX PARC,November 1997.

[8] Shuo-Yen Robert Li, Raymond W. Yeung, and Ning Cai. Linear net-work coding. In IEEE Transactions on Information Theory, vol. 49, pp. 371- 381, February 2003.

[9] T. Ho, R. Koetter, M. Medard, D. R. Karger, and M. Effros. The benefits of coding over routing in a randomized setting. In *ISIT*, July 2003.

[10] T. Ho, B. Leong, Y. Chang, Y. Wen, and R. Koetter. Network monitoring in multicast networks using network coding. In *ISIT*, 2005.
[11] T. Ho, B. Leong, R. Koetter, M. Mdard, M. Effros,and D. R. Karger. Byzantine modification detection in multicast networks using randomized network coding. In *ISIT*, 2004.
[12] S. Katti, D. Katabi, W. Hu, H. Rahul, and M. Medard. The importance of being opportunistic: Practical network coding for wireless environments. In *Allerton*, 2005.
[13] S.-Y. R. Li, R. W. Yeung, and N. Cai. Linear network coding. IEEE Trans. Inform. Theory, 49:371–381, Feb. 2003.
[14] A. Shokrollahi. Raptor codes. Submitted to IEEE Trans. Information Theory, 2004.
[15] N. R. Wagner. The Laws of Cryptography with Java Code. Available online at Neal Wagner's home page.
[16] J. Widmer, C. Fragouli, and J. Y. LeBoudec. Energy efficient broadcasting in wireless ad hoc networks. In NetCod, Apr. 2005.
[17] J. Widmer and J.-Y. LeBoudec. Network coding for efficient communication in extreme networks. In WDTN, Aug. 2005.
[18] Y. Wu, P. A. Chou, and K. Jain. A comparison of network coding and tree packing. ISIT, 2004.
[19] Y. Wu, P. A. Chou, and S.-Y. Kung. Information exchange in wireless networks with network coding and physical-layer broadcast. Technical Report MSR-TR-2004-78, Microsoft Research, Aug. 2004.
[20] R. Koetter and A. Vardy, "Factor graphs, trellis formations, and generalized state realizations," presented at the Institute for Mathematics and Its Applications, Aug. 6, 1999, available at http://www/ima.umn.edu/talks/workshops/aug12-13.99/koetter.html.
[21] F. R. Kschischang, B. J. Frey, and H.-A. Loeliger, "Factor graphs and the sum-product algorithm," IEEE Trans. Inform. Theory, submitted for publication.
[22] J. R. Roche, R. W. Yeung, and K. P. Hau, "Symmetrical multilevel diversity coding," IEEE Trans. Inform. Theory, vol. 43, pp. 1059–1064, May 1997.

Progression From Intermittent To 24x7 Mode Of Water Supply

Ms. M. H. Rana
Assistant Professor Civil Department, Silver Oak College of Engineering & Technology, Ahmedabad, Gujarat, India
mrunalini_rana@yahoo.co.in

***Abstract*- Clean drinking water and safe water supply is vital to our life. 24x7 water can deliver improved water quality and quantity to all urban consumers with a reduction in coping costs, health burden and also reduce burden on water recourses. The problem with intermittent water supply is that it leads to serious public health issues and weakens the system by leakages. Water supply system efficiency is of primary importance in designing either new water distribution networks or expanding existing ones. Water distribution network, a hydraulic infrastructure consisting of elements such as pipes, tanks, reservoirs, pumps, and valves etc., is crucial to provide water to the consumers. Design optimization of water distribution networks has been thoroughly researched over the past few decades due to its computational and engineering complexity. The majority of the studies dealt with least-cost optimization. In the light of above, aim of the present study is to assess the water supply scheme for 24x7 water supply using EPANET - a computer based program that performs extended period simulation of hydraulic and water quality behavior within pressurized pipe networks.**

***Keywords*- Water supply system, water distribution network, intermittent water supply, continuous water supply, EPANET.**

I INTRODUCTION

24x7 supply is achieved when water is delivered continuously to every consumer of the service 24 hours a day, every day of the year, through a transmission and distribution system that is continuously full and under positive pressure. Break-up of minimum domestic water supply standard as per CPHEEO manual:

II GENESIS OF RESEARCH

Domestic water use/demand is a complex function of socio-economic characteristics, climatic factors and public water policies and strategies (Babel et al. 2007). Water consumption is defined as the amount of water actually supplied (or estimated to be supplied) for some (legitimate) purpose whereas demand indicates the amount of water estimated to be required for the purpose.

Gross consumption is inclusive of distribution losses, which include leakage and wastage that frequently reach values of 30% or even 40% from all drinking water supply system (Araujo et al. 2006). Unaccounted for water (UFW) which is also known as non-revenue water is defined as the difference between water produced and supplied to the distribution system. Definition of UFW applicable to localities where metering is practised, is production minus metered use and water sold (Indo–US Financial Institutions Reform and Expansion Project—Debt Market Corporation FIRE (D) 2000).

Table 1 Break-up of minimum domestic water supply

Use/Activity	Amount	Percentage of Total
Drinking & Cooking	15	10%
Bathing, Washing clothes, vessels & floor	75	55%
Flushing toilet	45	35%
Total	135	100%

Source CPHEEO Manual

The term "UFW" refers basically to water losses and leaks not accounted for, including distribution losses, illegal connections and water theft (Hueb et al. 1999). Water which is not accounted for separately like distribution leakages from main valves, service pipe connections etc. and unmetered supplies are the distribution losses. Leakage from trunk mains and service reservoirs can often be measured directly, but this is not the case with distribution system. For practical purposes, the best measure of leakage is obtained from minimum night flow (during which no legitimate water requirement is anticipated) modified by subtracting the known metered consumption (Andey and Kelkar 2007; Tabesh et al. 2008). Water consumption by a community is dependent on a number of factors like season, climate, cultural habits and local customs. The seasonal variation in the daily demand may vary from ±10% to 30% of the average daily demand for the year. The hourly variations in water demand during the day is much greater compared to the average daily demand. Generally water requirement is more during morning and evening hours than the noon demand. As far as the design of distribution system is concerned, hourly variation in demand has an influence on the residual pressures in the system. These fluctuations

in demand are accounted for by peak factor at the design stage. A water distribution system is designed to supply the maximum hourly demand. In developing countries the water distribution systems are designed for continuous water supply (CWS) with peak factors in the range of 2.0 to 3.0 (CPHEEO 1999) where as in actual practice due to non-availability of adequate quantity of water at source and financial constraints, it is not practically possible to operate drinking water systems for 24 h/day (Rajiv 2003). So despite considerable negative impacts, the distribution systems are operated on intermittent mode, resulting in inequitable water flow and pressures in the system (Vairavamoorthy and Elango 2002; Totsuka et al. 2004).

Intermittent water supply (IWS) creates high peak factors in the distribution system which causes low pressures at a number of locations. People are required to store water in their houses for the whole day consumption. Most people living in cities would like to be connected to a 24-h supply of piped water Joshi et al. 2002). In most Asian cities, less than 30% of the residents are enjoying 24-h water supply. Low service coverage and intermittent supply have become a norm rather than exemption (Seetharam 2005).

III THE CURRENT SITUATION AND CHALLENGES OF INTERMITTENT WATER SUPPLY

The supply of water in Indian towns and cities may last for just one or two hours every day or every other day; it could be even less in certain locations. The water that is supplied is not potable, that is, it is not of sufficient quality to be drunk straight from the tap without exposing oneself to the risk of waterborne diseases and infections. The supply may be of insufficient pressure to flow directly from taps even at a ground floor level, let alone taps in rooms or apartments on the first or higher floor of buildings. Poor water service levels have led to consumers adopting expensive coping strategies that include installing underground storage tanks, suction pumps on water mains or overhead tanks, boiling water or using household filters. Those without a connection have to queue at stand posts, sometimes with belowground-level pipe outlets (pit taps) to access sufficient water pressure with the additional burden of often not knowing when water may come. Under intermittent service, when pumping stops and the pressure in the pipes drops, water that had been leaking out of faulty joints or holes can be sucked back in. This water could be polluted by wastewater seeping from toilets, septic tanks, domestic drains, and road drains. Intermittent water supply thus not only leads to the water provider delivering polluted water, it also leads to increased pumping costs, reduced lives of pipes and connections due to wide changes in pressure, and an inability to know how the network is operating as meters fail to operate effectively.

Despite low levels of service, the arguments against the idea of continuous 24x7 water have been strong: “We don’t have enough water in a water-scarce country to supply continuous water”; “It will cost too much when so many people are poor and tariffs are already too low”; “We have intermittent power supply so how can we expect to have continuous water supply?”; and “Our cities are growing too quickly to support continuous water”.

IV METHODOLOGY TO BE ADOPTED

- Collection of data like latest population from census record for the area
- Study existing water supply scheme and present water distribution network scenario
- Forecasting the future population growth
- Preparing the new network map of the whole area
- Designing the water supply network for 24x7 using EPANET
- Assessing the advantage of continuous water supply from intermittent

V IMPLEMENTING 24X7 SUPPLY

Phase A: Preparation

The first task in the preparation phase was to determine the number of potential consumers and their likely demand for water, in addition to assessing the condition of the existing pipes, followed by hydraulic design of the new system. Fifteen weeks had been allotted for this task, and it was achieved with a short delay (an additional six weeks had been allowed for such flexibility). “It was the most difficult stage as there was no information available. There were no bulk water meters, no household meters; nobody knew where the water was going. They were saying the losses could be 40 percent to 50 percent but that was simply a guesstimate.”

Phase B: Implementation

In the demonstration zones, install an all new pipe network, including service connections, along with bulk and consumer metering, pressure management, and monitoring devices. A billing and customer service system was established along with a performance monitoring system. Attention to detail was required on the house connections. The ferrule connection, where the smaller house connection pipe is joined to the water main in the street, is often a source of leaks. The high quality electro-fusion ferrules, and similarly high quality imported brass water meters within a plastic meter box for protection, to ensure performance.

Phase C: Operation

Over a period of months, the new water distribution pipes were brought into service, new household connections were made, and the new system was brought into operation with full metering of bulk supply and household metering of all connections. The operations period officially commenced in all three cities. "The first consumers received 24-hour supply three months early and the pessimism in the consumers' minds was killed automatically, very fast." Households received continuous water supply at the design pressure, water in taps inside their homes, even in third storey apartments, 24 hours a day, seven days a week. A good database on the improved water network which is important for good operations, with data loggers used to record regular measurements and understand system performance. Water now came at a pressure which allowed middle-income households to fill their roof storage tanks (just in case) without any need to spend electricity on booster pumps. Pumps to suck water out of the mains became redundant. It is, however, reported that only about 30 - 40 percent of the ground-level sump tanks have been bypassed and left unused so far, even though householders were advised to do so. The water which came out of the pipes was now potable (additional chlorination facilities were built to ensure that the water was properly disinfected), so there was no value in allowing it to become polluted again through storage in underground house sumps. Potable water supply also made it possible to dispense with household treatment systems though not all had done so.

VI 24X7 WATER IS ACHIEVABLE

Reportedly, some of those who were most against the demonstration project, particularly since it involved a foreign operator, held out against the offered improvements. Initially one ward in one town rejected the idea of improved water supply. Then it was just two streets that refused, and finally just one individual objected, until the normality of 24x7 continuous water supply and its benefits became too apparent. Then he, too, connected to the system.

The largest movement towards normality came from the lowest income households which had traditionally had to queue at distant stand posts in the early hours of the morning, waiting for water to come. However, the stand posts were shut down because all poor households opted for household connections. This is one of the most important lessons from the project with respect to pro-poor advocacy arguments. This gave the poorest families immediate 24x7 access to water, without having to carry drinking water in buckets, removing a potential source of contamination. Continuous access also delivered hygiene benefits in facilitating hand washing before food preparation and meals, in addition to the convenience and dignity aspects.

Observation made for twin city Hubli and Dharwad, Karnataka (INDIA) a comparison from Intermediate to Continuous Water Supply.

VII DESIGN OF WATER DISTRIBUTION NETWORK USING EPANET

EPANET is a computer program that performs extended period simulation of hydraulic and water quality behaviour within pressurized pipe networks.

A network consists of pipes, nodes (pipe junctions), pumps, valves and storage tanks or reservoirs. EPANET tracks the flow of water in each pipe, the pressure at each node, the height of water in each tank, and the concentration of a chemical species throughout the network during a simulation period comprised of multiple time steps. In addition to chemical species, water age and source tracing can also be simulated.

Table 2 A comparisons from Intermediate to Continuous Water Supply.

Parameters	Situation before	Situation after intervention
Hourly supply	2 hour in 3 to 7 days	24x7
Volume of water supplied in Mld	22.14	18.24
Average pressure in distribution system (m)	0-5 m	17.70 m
Population served	1,80,000	1,80,000 by 2,40,000 individual connections
No. of public fountains	433	Zero, all end-users provided with individual connections with meter
Losses as % of input	More than 50 %	7%
Metering	None	100%
Computerized records	None	100%
Customer complains response time	Not applicable	24 hrs
Billing collection	Not applicable	Approx. 80 %
Customer service	Not existed	Available for 24 x 7

Source: **www.wsp.org/wsp/sites/wsp.org/files/.../WSP_Karnataka**

EPANET is designed to be a research tool for improving our understanding of the movement and fate of drinking water constituents within distribution systems. It can be used for many

different kinds of applications in distribution systems analysis.
Sampling program design, hydraulic model calibration, chlorine residual analysis, and consumer exposure assessment are some examples. EPANET can help assess alternative management strategies for improving water quality throughout a system.
These can include:

- Altering source utilization within multiple source systems,
- Altering pumping and tank filling/emptying schedules,
- Use of satellite treatment, such as re-chlorination at storage tanks,
- Targeted pipe cleaning and replacement.

One typically carries out the following steps when using EPANET to model a water distribution system:

Draw a network representation of your distribution system or import a basic description of the network placed in a text file

1.Edit the properties of the objects that make up the system
2.Describe how the system is operated
3.Select a set of analysis options
4.Run a hydraulic/water quality analysis
5.View the results of the analysis

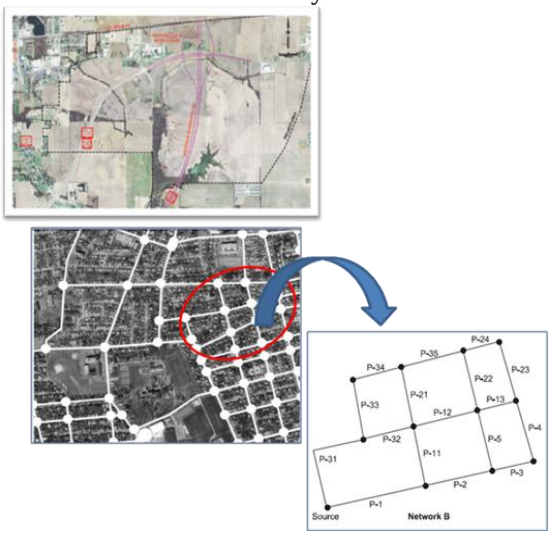

Fig.1 Network diagram and design using EPANET

EPANET, a widely used water distribution network simulation model, is used in this study to deal with both the steady state and extended period simulation and is linked with a powerful optimization algorithm, Shuffled Complex Evolution or using Differential Evolution. This deals with a set of population of points and searches in all direction within the feasible space based on objective function. This method is applied for the design of a cost effective water distribution network. The findings of this study show that SCE and DE is computationally much faster when compared with other also widely used algorithms such as GAs, Simulated Annealing, GLOBE and Shuffled Frog Leaping Algorithms. Hence, SCE and DE is a potential alternative optimization algorithm to solve water distribution network problems.

VIII CONCLUSION

24x7 SUPPLY DELIVERS BETTER QUALITY WATER FOR PUBLIC HEALTH.

High levels of bacterial contamination are experienced in the first 10 minutes of repressurization of an intermittent system, in some cases persisting for up to 20 minutes. Maintaining full pressure removes that risk.

24x7 supply gives significantly better service to all consumers.

Access to clean water with improved quantity, timing, and pressure, including effective service to supply pipe 'tail ends'.

24x7 supply revolutionizes service to the poor.

Consumers can access more water for improved health and hygiene while saving time in queuing and carrying, and gainfully using the time thus saved for employment opportunities.

24x7 supply converts household coping costs into resources for the service provider.

Coping costs that consumers need to incur are reduced; they pay for a better service.

24x7 supply reduces the burden on water resources.

Continuous supply reduces water wastage arising from overflowing storage systems and open taps. It saves on stored household water that is discarded when new supply comes in. Because the network is renewed where needed, it also reduces losses arising from leaks in the old pipes.

24x7 supply delivers effective 'supply management' and 'demand management'.

Continuous supply makes possible the effective management of leakage through pressure management and flow measurement. Water conservation is also encouraged through metering and price signals via a volumetric tariff to consumers.

24x7 supply enables improved efficiency of service provision.

Operational efficiencies are achieved because of a reduced need for valve men, and a conversion of these jobs into more efficient ones of meter reading and customer care. It also makes possible the management of illegal connections.

REFRENCES

[1]CPHEEO-Central Public Health and Environmental Engineering Organization Manual on water supply and treatment, 3rd edn. Ministry of Urban Development and Poverty Alleviation, Govt. of India, New Delhi, 1999

[2]www.wsp.org/wsp/sites/wsp.org/files/.../WSP_ Karnataka
[3]Richard Francey and Anand Jalakam, Water and Sanitation Program Report, The Karnataka Urban Water Sector Improvement Project, 2010.
[4]A. Vasan and Slobodan P. Simonovic, Optimization of Water Distribution Network Design Using differential Evolution, Journal of Water Resources Planning and Management,, Vol.136, No.2, 2010.
[5]Shie-Yui Liong and Md.Atiqzzaman, Optimal Design of Water Distribution Network Using Shuffled Complex Evolution, Journal of the Institution of Engineers, Vol.44, No.1, 2004.
[6]Andey SP, Kelkar PS Performance of Water Distribution System during Intermittent versus Continuous Water Supply, JAWWA, Vol.8, No.99, pp. 99-106, 2007.
[7]Lewis A. Rossman, EPANET 2 users manual

Compressive Strength and Modulus of Elasticity of Self-Compacting Concrete

Anant Patel[1],Prashant Bhuva[2],Elizabeth George[3],Darshana Bhatt[4]
[1,2](*PG Students, Dept. of Structure Engg. B.V.M Engg., College, V.V.Nagar, Gujarat, India.)*
[3,4](*Professors , Dept. of Structure Engg. B.V.M Engg., College, V.V.Nagar, Gujarat, India.)*
[1]arp_925@yahoo.co.in
[2]prashant_civil31@yahoo.co.in
[3]pmgeorge02@yahoo.com
[4]darshanabvm@gmail.com

***Abstract*- The topic on 'Compressive Strength and Modulus of Elasticity of Self Compacting Concrete' contain trial mixes for SCC with effects of admixtures, and various content of cement and Fly Ash. The study involves 'Relative Slump Cone Test' for fixing the w/p ratio, analysis of hardened properties of concrete with compressive strength testing machine and the study of modulus of elasticity.**

***Keywords*- Compaction, Compressive Strength, Fly Ash, Super Plasticizer, Viscosity Modifying Agent, Water/Paste Ratio.**

I INTRODUCTION

SCC has been developed to ensure adequate compaction and facilitate placement of concrete in structures with congested reinforcement and in restricted areas. SCC was developed first in Japan in the late 1980s to be mainly used for highly congested reinforced structures in seismic regions. As the durability of concrete structures became an important issue in Japan, an adequate compaction by skilled labours was required to obtain durable concrete structures.

The requirement led to the development of SCC and its development was first reported in 1989, as in [11]. SCC can be described as a high performance material which flows under its own weight without requiring vibrators to achieve consolidation by complete filling of formworks even when access is hindered by narrow gaps between reinforcement bars, as in [19].

The mix proportioning of self-compacting concrete is shown and compared with those of normal concrete and R D (Roller Compacted concrete for Dams) concrete, as in [16]. The aggregate content is smaller than conventional concrete that requires vibrating compaction.

SCC can also be used in situations where it is difficult or impossible to use mechanical compaction for fresh concrete, such as underwater concreting, cast in-situ pile foundations, machine bases and columns or walls with congested reinforcement. The high flowability of SCC makes it possible to fill the formwork without vibration, as in [5]. Since its inception, it has been widely used in large construction in Japan, as in [12]. Recently, this concrete has gained wide use in many countries for different applications and structural configurations.

The SCC nature shows the basic concept. The method for achieving Self-Compactability involves not only high deformability of paste or mortar, as shown in (Fig. 1). But, also resistance to segregation between coarse aggregate and mortar when the concrete flows through the confined zone of reinforcing bar. Homogeneity of SCC is its ability to remain un-segregated during transport and placing.

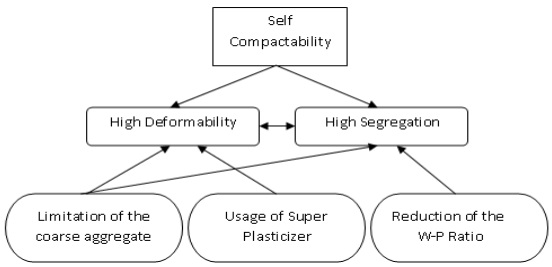

Fig. 1 SCC Nature

II DESIGN OF SCC

2.1 General

The first step of the process is to fix the W/P ratio by performing 'Relative Slump Cone Test', and then optimizing the dosage of Super-Plasticizer by 'Marsh Cone Test' keeping fixed percentage of VMA (0.31%).

2.2 Determination Of W/P Ratio For The Self Compacting Concrete.

Flow cone to determine relative slump flow:

Tests are conducted on mortar (cement, Fly Ash, sand and water) for different water/powder ratios (usually 1.1, 1.2, 1.3 &1.4) using a flow cone, as shown in (Fig. 2). The water powder ratio is based on an absolute (solid) volume. As per different trial mix, the test results of flow cone are shown in Table 1

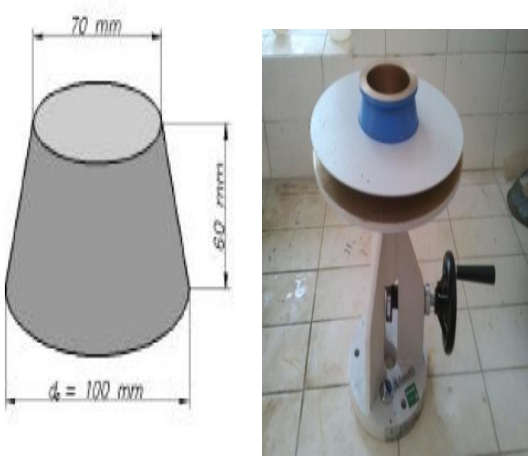

(a) (b)

Fig. 2 Flow Cone

Table 1 Test Results For Flow Cone

Trial Mix	Flow Diameter with Different Water/Powder Ratio				
	1.0	*1.1*	*1.2*	*1.3*	*1.4*
B1	SF	Zero Slump	160	190	210
B2	SF	SF	Zero Slump	160	220
D1	110	150	200	225	-
D21	Zero Slump	135	175	-	-
D22	SF	110	150	190	-
D3	SF	SF	120	160	210
SF- Shear Failure and Flow Diameter in mm					

2.3 Test Conducted for Fresh Properties of Self Compacting Concrete

There are three key fresh properties of SCC for mix design purposes in the lab and for compliance purposes on site.

- Filling ability,
- Passing ability and
- Resistance to segregation

Based on the EFNARC Guidelines, slump flow, visual stability, L-box, U-box, V-funnel, J-ring, filling box and column segregation tests are some of the available testing methods used to evaluate fresh properties.

2.4 Mix Design

The characteristics of powder and super plasticizer largely affect the mortar property and so the proper water powder ratio and super plasticizer dosage cannot be fixed without trial mixing at this stage. Therefore, once the mix proportion is decided, self-compact ability has to be tested by slump-flow L-box and v-funnel tests. Test results are shown in Table 2 and 3.

Ingredients used in mix design: The mix contains Cement (OPC 53), Fly Ash (Grade F), Polycarboxylic Ether based Super Plasticizer, Viscosity Modifying Agent, Coarse Aggregate (10-20mm), Fine Aggregate (Sand Zone II), Potable Water.

Laboratory test are conducted for the observation of the specific gravity of different ingredients with proper care. All the equipments used are of standard quality and performing well. The Ingredient values are as:

- SP. Gravity for C.A - 2.92
- SP. Gravity for F.A -2.6
- SP. Gravity for Fly Ash - 2.3
- SP. Gravity for Cement - 3.15
- Entrapped Air - 2%
- Voids – 0.98

Table 2 Trial Mixes

Trial mixes	W/P	Ceme-nt	Fly Ash	C.A 10mm	F.A	Water
B1	1.1	300	250	751.88	814.54	224.32
B2	1.2	300	200	798.91	865.48	218.62
D1	1.1	400	250	673.46	729.58	259.23
D21	1.0	400	200	762.83	826.39	213.94
D22	1.2	400	200	735.19	735.19	256.72
D3	1.3	400	150	774.93	774.93	249.86
SP - 0.8% and V.M.A - 0.31% of Cementious material						

Table 3 SCC Fresh Properties

Trial mixes	Slump		V-Funnel		L-Box	
	T50 in Sec	*Dia mm*	*T0 in sec*	*T5 in Sec*	*h2/h1*	*Time in Sec*
B1	2.0	650	5.0	8	1.0	4.36
B2	4.0	640	6.0	7	0.9	6.0
D1	1	770	3.4	3.96	0.92	1.21
D21	N.A	N.A	N.A	N.A	N.A	N.A
D22	1.43	780	3.23	4.0	0.8	1.63
D3	1.33	650	3.79	4.81	0.875	3.03

III TEST RESULTS

3.1 Determination of Compressive Strength

The cubes are cast having size 150 x 150 x150mm for different trial mix and are tested for the compressive strength.

The 7-days and 28-days strength are conducted, which are shown graphically, as in (Fig.4).

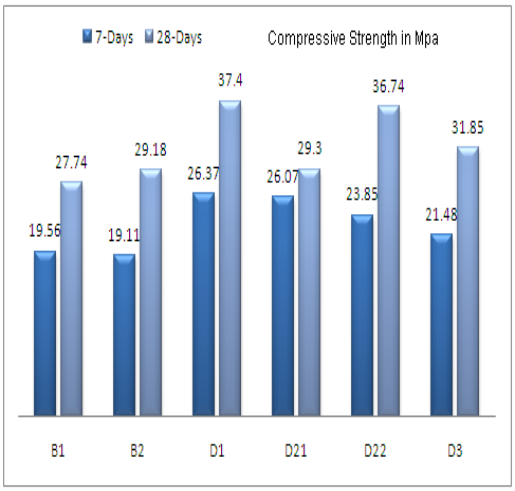

Fig. 4 Test Results for Compressive Strength

3.2 Test Results for Modulus of Elasticity

Modulus of elasticity is the property that influences the safety, durability and service life of reinforced concrete. In addition, it also gives indication of density and stiffness of aggregate paste matrix of SCC.

Table 4 Modulus Of Elasticity

Sr. No	Trial Mix	Modulus of Elasticity N/mm²
1	B1	24673
2	B2	26258
3	D1	18486
4	D21	20825
5	D22	20901
6	D3	17505

The graphs shows modulus of elasticity, conducted for different cylinders, cast for trial mixes.

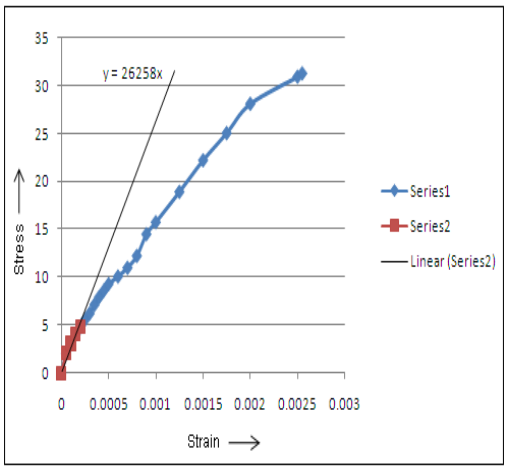

Fig. 5 Modulus of Elasticity for Trial Mix B2

Fig. 6 Test Setup for Modulus of Elasticity

IV CONCLUSION

From the test results conducted for relative slump cone test, compressive strength and Modulus of Elasticity following conclusions are drawn:

- From Table 1 and 3 it is seems that when w/p ratio is lower flow obtained for concrete is also lower and it is not up to the requirement of SCC. Therefore, when flow obtained is lower it is necessary to increase the w/p ratio for given cement and fly ash content.
- It is observed that having higher cement content is giving more cohesive mix and also having high compressive strength.
- It is seen that D21 is not fulfilling SCC requirement for fresh concrete. But, D22 with same cement and fly ash content with higher w/p ratio and higher water fulfills SCC requirements and also giving Compressive strength at 28-days.
- Modulus of Elasticity of different mixes as obtained in Table IV shows that they are comparable with normal cement concrete.

ACKNOWLEDGMENT

We sincerely thank our advisors Prof. Elizabeth George and Dr. Darshana R Bhatt (B.V.M Engg. College V.V.Nagar), for their guidance, suggestions, and continuous support throughout our research work. Our greatly thanks to Principal Dr. F.S.Umrigar Sir and Dr.A.K Verma H.O.D of Structure Dept. We also thankful for the sincere support given by the Engineering Experts at Ambuja Knorwledge centre-Baroda. We greatly appreciate all the support that they had been given to us.

REFERENCES

[1] Anant Patel, “Hardend Properties of Self Compacting Concrete”,

[2] Second National Conference on Emerging Vistas of Technology in 21st Century, pp. 37-44. 4-Dec (2010)

[3] Bouzoubaa, N., and Lachemi, M., "Self-compacting concrete incorporating high volumes of class F fly ash: preliminary results", Cement and Concrete Research, Vol. 31, pp. 413-420. (2001).

[4] Dr. Hemant Sood1, Dr. R. K. Khitoliya and S. S. Pathak, "International Journal of Recent Trends in Engineering", N.I.T.T.T.R; Chandigarh, INDIA Vol.1, No. 6, May (2009)
[5] EFNARC, "Specifications and Guidelines for Self-Compacting Concrete", EFNARC, UK (www.efnarc.org), pp. 1-32.February (2002),
[6] Khayat, K.H., Assaad, J., Daczko J., "Comparison of Field-oriented Test Methods to Assess Dynamic Stability of Self-Consolidated Concrete", ACI Materials Journal, V. 101, No. 2, March –April, pp. 168-176. (2004)
[7] Krieg, W., "Self-Compacting Concrete: Definition, Development, and Applications", A Technical Paper Presented in the Meeting of the ACI, Saudi Arabia Chapter, Eastern Province, October. (2003).
[8] Mata, L. A., "Implementation of Self-Consolidating Concrete (SCC) for Prestressed Concrete Girders", MS Thesis, North Carolina State University, Nov (2004).
[9] Miao Liu Self-compacting concrete with different levels of pulverized fuel ash by Department of Civil, Environmental and Geomatic Engineering, University College London, London WC1E 6BT, United Kingdom. 23-November (2009).
[10] Mindess, S., J. F. Young, and D. Darwin, "Concrete", Second Edition, Prentice Hall (2003).
[11] Okamura, H. and Ouchi, M., "Self-compacting concrete-development, present and future", Proceedings of the First International RILEM symposium on Self-Compacting Concrete, pp. 3-14. (1999).
[12] Okamura, H. and Ouchi, M., "Self-compacting concrete", Journal of Advanced Concrete Technology, Vol. 1, No. 1, pp. 5-15. April (2003).
[13] Ozkul, M. H. and A. Dogan, "Properties of fresh and hardened concretes prepared by N-vinyl copolymers", International Conference on Concretes, Dundee, Scotland (1999).
[14] Paratibha Aggrawal, Rafat Siddique, Yogesh Aggrawal, Surinder M Gupta, "Self-Compacting Concrete - Procedure for Mix Design", Leonardo Electronic Journal of Practices and Technologies, Kurukshetra, (Haryana), India, Issue 12, Jan-June (2008).
[15] Prashant Bhuva, "Evaluation of Properties of Fresh Self Compacting Concrete", Second National Conference on Emerging Vistas of Technology in 21st Century, pp. 27-36. 4-Dec (2010)
[16] R.N. Kraus a, T.R. Naik a, B.W. Rammeb, Rakesh Kumar "Use of foundry silica-dust in manufacturing economical self consolidating concrete" by a UWM Center for By-Products Utilization, Department of Civil Engineering and Mechanics, University of Wisconsin-Milwaukee (UWM), P.O. Box 784, Milwaukee, WI 53201, USA Environmental Department, We Energies, Milwaukee, WI 53203, USA. 29-April
[17] Subramanian, S. and D. Chattopadhyay, "Experiments for mix proportioning of self-compacting concrete", The Indian Concrete Journal, pp.13-20 (2002).
[18] Su N., Hsu K C., and Chai H W., "A simple mix design method for self compacting concrete", Cement and Concrete Research, Vol. 31, pp. 1799-1807. (2001).
[19] Whiting, D, "Effects of High-Range Water Reducers on Some Properties of Fresh and Hardened Concretes", Portland Cement Association, R & D Bulletin 061.01T (1979).
[20] Zhu W., Gibbs C J., and Bartos P J M., "Uniformity of in situ properties of self compacting concrete in full-scale structural elements", Cement & Concrete Composites, Vol. 23, pp. 57-64. (2001).

Analysis Of Speech Of Depressed Person

Mohammed Vayada[1],Vimal Nayak[2],Amit Agrawal[3]
[1,2,3]*EC Dept, Silver Oak College of Engineering & Technology, Ahmedabad, Gujarat, India*
[1]vayada.mohammed@gmail.com
[2]vimalhnayak@yahoo.com
[3]a.agrawal88@gmail.com

***Abstract*-Acoustic properties of speech have previously been identified as possible cues to depression, and there is evidence that certain vocal parameters may be used further to objectively discriminate between depressed and normal speech. In this research, these questions are addressed empirically using classifies configurations employed in emotion recognition from speech, evaluated on depressed/neutral speech database. Results demonstrate that detailed spectra features are well suited to the task; speaker normalization provides benefits mainly for less detailed features and dynamic information appears to provide little benefit. In this research first voiced part is separated from whole speech. The Spectral Entropy was extracted from the collected voiced speech samples using the method of the spectrum analysis.**

***Keywords* - Depression, Power spectral Density, Spectral Entropy, Speech, Voiced/Unvoiced.**

I INTRODUCTION

Our life under the pressure of social competition today may cause some people to feel stressful, having a hard time catching up on things every day of their lives rushing. Some have thought to approach the edge of hard-survival time which may affect their feelings, spirit and mind temporarily and / or permanently [1].

Without being properly supervised by the care taker or to obtain appropriate treatment in time, such damage could be more serious if the person suffers from depression. How to know when this strike would be the first symptoms to start with the first step. People at risk of such a disorder may feel unhappy and depressed, isolated, lack of energy, loss of an aperitif, and even though no hope in life and finally give their lives. Suicide could be the chance for someone severely depressed at the end-their life unpleasant and treatment effort could be powerless to that mindset. Identify depressive people among others who are normal is a critical problem in clinical practice. To assess the psychiatric status of the subject, the practitioner should involve the collection of information about the balance sheet profile, visit the hospital records, crime-related reports and oversees health care hotline. Clinical judgment is another important procedure that is based largely on information data processing and interpretation of results were analyzed in the clinical perspective. This task to acquire clinical data and psychiatric diagnosis is the procedure time and should be treated with clinical expertise. Another in some way to address this important clinical practice must be discussed and proposed. The rapid assessment of symptoms of the subject by the psychiatrist is necessarily required for decision making on the subject real serious category is part of an appropriate treatment to be accorded to this subject. The emotional speech samples were studied for changes in the acoustic characteristics caused by emotional problems, depression. Speech was reported to be related to emotional and mental condition a loudspeaker while talking, which might suggest an idea of how to predict the level of severe affective disorders in a patient which affects the production of speech speaker and mediation in the results of speech. In the point of view of speech, the height of high and low speech sounds depends on a change in fundamental frequency over the time interval to meet the glottal wave generated directly from the dynamic supply system in the speech production. Change in the range of fundamental frequency, energy shift and the spectral energy ratios on the frequency bands were studied and reported as predictors of the mental state associated with depression. Methods for estimating the energy of the speech signal are varied and diverse, as decided by the researchers to choose and implement. An estimation method known is the estimate of entropy of speech and how to estimate this function is convenient for implementation. Entropy is defined as the average amount of information per message which refers to the amount of meaningful speech information leads to the listener. This speech is the main objective to be described on its relevance to the classification of diagnostic symptoms [2].

II METHODOLOGY

2.1 Database and Preprocessing

The database consists of patients who were categorized as either depressed or normal by a clinician who was not involved in the research project. All speech recordings were made on mono channel. All voice recordings were digitized with a higher sampling rate of 16 kHz for better sound quality and converted to10 kHz. These recordings were then edited using the NCH wave pad audio digital editor by removing the interviewer's voice,

removing long pauses that are present for more than 0.5 second and removing background noises such as door slams, sneezing and paper rustling sounds[3].

Speech signals are comprised of voiced, unvoiced, and short silence segments that are mixed and combined together. According to Ozdas, voiced, unvoiced and silence speech samples can be estimated by segmenting the sampled signals based on their energy values at different levels of the Wavelet Transform (WT). Voiced speech samples exhibit a quasi-stationary behavior and are composed of low frequency characteristics. On the other hand, unvoiced speech samples exhibit noise-like behavior and contains more high frequencies. The sampled signals were separated into segments and for each segment; the energy was calculated for each of several different band levels.

Energy for each band was obtained by calculating the Discrete Wavelet Transform (DWT) at each frequency band levels. These bands represent a set of band pass filters as shown in Table 1.

Table 1 Frequency range for each band levels

Band level	-3dB band pass filter limits
1	2500 – 5000
2	720 – 2340
3	320 – 1080
4	160 – 540
5	80 – 260

Lower bands allow higher frequency content and filter out low frequency information while higher bands capture the lower frequency information.

III FEATURE EXTRACTION

In this section of paper, only the voiced speech is further analysed for feature extraction. The procedure to obtain entropy features is described as:

1. Windowing the voiced speech into 25.6ms length frames of speech signal.
2. Multiplying each speech frame with "Hamming Window" in order to reduce the edge effect of segmentation due to un-matching between the beginning and ending point of the windowing frame and the zero-crossing point in speech signal.
3. Estimating the speech spectrum by calculating Discrete Fourier Transform (DFT) for each segment with N-point FFT of 256 samples.
4. Approximating the probability density function (PDF) for each frame of speech by dividing the magnitude of individual frequency component by the total sum of all spectral magnitude over a0-5KHz frequency range.
5. Estimating the entropies of the occupied 1.25 KHz frequency sub-bands of spectral PDF by following the calculation of Equ. (1)
6. Calculating the mean and standard deviation of each extracted sub-band entropy for every 200 samples to form a 8xM input feature matrix to classification, where M is number of means
7. Evaluating the class separation power of the entropic means and SD's by measuring the F-ratio for each feature, which is a ratio of between-class variance and within-class variance, and ranking all tested features in order based on their F-ratio measure
8. Calculating the discriminating score, which is a separating distance with respective to class means, for each feature and combination of selected feature

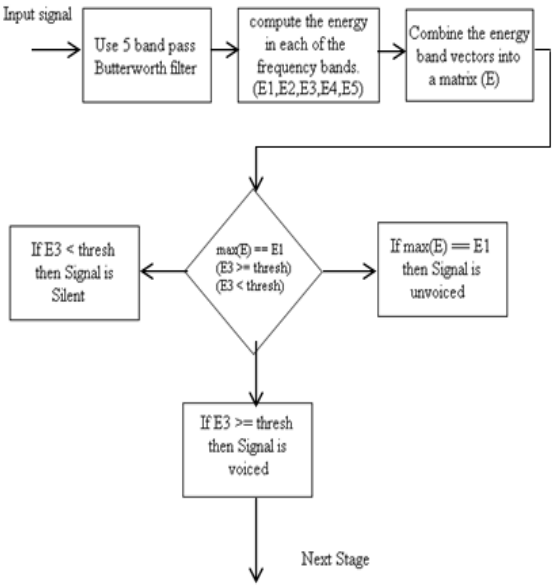

Fig.1 Block diagram for voiced, unvoiced and silent detection

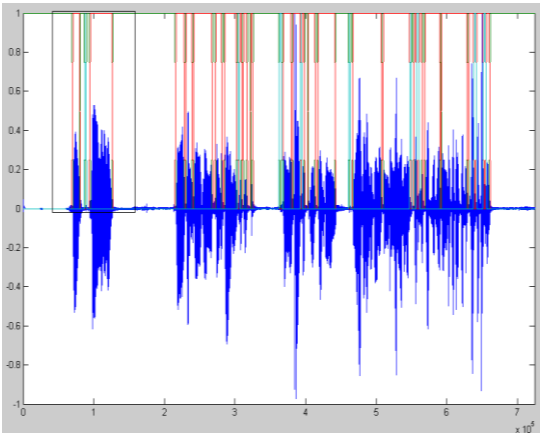

Fig.2 voiced, unvoiced and silent part of speech

$$H = \sum_{i=1}^{N} s(i) * \log [s(i)] \qquad ..Equ.(1)$$

Where H is the estimate of entropy for each speech frame, $s(i)$ represents the spectral PDF of the *ith* frequency component and N is the number of all frequency components in spectrum.

IV FEATURE CLASSIFICATION

The Support Vector Machine (SVM), which outperforms most other classification systems in a wide variety of applications, has been used in this study for performance validation. It achieves relatively robust pattern recognition performance using well established concepts in optimization theory. SVM separates an input $x \in \boldsymbol{R}^d$ to two classes. A decision function of SVM separates two classes by $f(\boldsymbol{x}) \gtrless 0$ or $f(\boldsymbol{x}) \gtrless 0$. The training data which is used in training phase is $\{ \boldsymbol{xi}, \boldsymbol{yi} \}$, for $i = 1,\ldots l$ where $\boldsymbol{xi} \in \boldsymbol{R}^d$ is the input patternor the ith sample and $yi \in \{-1, 1\}$ is the class label. Support Vector Classifier maps $\boldsymbol{xi}$ into some new space of higher dimensionality which depends on a nonlinear function $\phi(\boldsymbol{x})$ and looks for a hyper plane in that new space. The separating hyper plane is optimized by maximization of the margin. Therefore, SVM can be solved as the following quadratic programming problem [6],

$$\max_{\alpha_i}\{\sum_{i=1}^{l} \alpha_i - 12\alpha i\alpha j yiyjK(xixj)\} \quad ..Equ.(2)$$

Subject to $0 \le \alpha_i \le C$ and

$$\sum_{i=1}^{l} \alpha_i y_i$$

Where C is a parameter to be chosen by user, a larger C corresponding to assigning a higher penalty to errors, and $\alpha \ge 0$ are Lagrange multipliers [4].

When the optimization problem has solved, system provides many a ≥ 0 which are the required support vector. Note that the Kernel function $K(x_i x_j) = \phi^T(x_i)\phi(x_j)$ where $\phi(\bullet)$ is a nonlinear operator mapping input vector $\boldsymbol{xi} \in \boldsymbol{R}^d$ to a higher dimensional space. In addition, other kernels can also be applied. Classification consists of two steps: training and testing. In the training phase, SVM receives some feature patterns as input. These patterns are the extracted speech features represented by N feature parameters that can be seen as points in N-dimensional space. In this study, eight features comprised of four means and four SD's were formed as input feature matrix which is multi-dimensional. Therefore, the classifying machine becomes able to find the labels of new vectors by comparing them with those used in the training phase. In training state, the 50% of all feature samples was randomly selected as the input feature model to SVM. Then, the rest 50% of randomized samples was used in validating state. For every feature model, the cross validations have been completed for approximately 100 times. Each feature model as input feature to SVM was formed by adding one more ranked feature every time when new feature model is validated. By using the same validating procedure, the performance of validation on same feature models by linear classifier was determined as well. The tendencies of performance evaluated from both SVM and linear classifiers are provided in next section [5].

V RESULTS AND DISCUSSION

Estimated entropy can evidently represent two distinguishing sections in speech signal: the energy concentrated voiced speech segment and the flat less energy unvoiced speech segment. The separating boundaries between voiced and unvoiced segments in speech signal can be obviously observed at the shifts in entropy value, reflecting as the end-points of voiced and unvoiced segments in speech signal.

In addition, the class discriminant distance was determined on the basis of Fisher's discriminant function, which helps project the dimensional feature set onto a single feature dimension. Fig. 3 show the discriminant distances between two speech classes in which two and more entropy features were taken in account of statistical measurement. When the dimension of entropy feature model is increased, the distance between discriminant scores from two classes is, consequently, longer. Fig. 4 indicates the decision boundary drawn on two classes of the identified samples via SVM classifier.

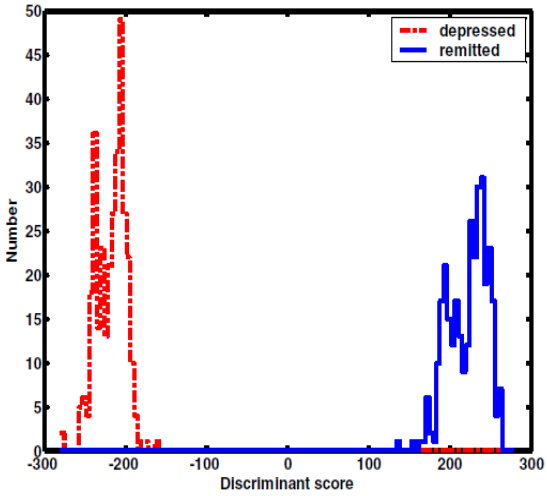

Fig.3 Multivariate discriminant distance

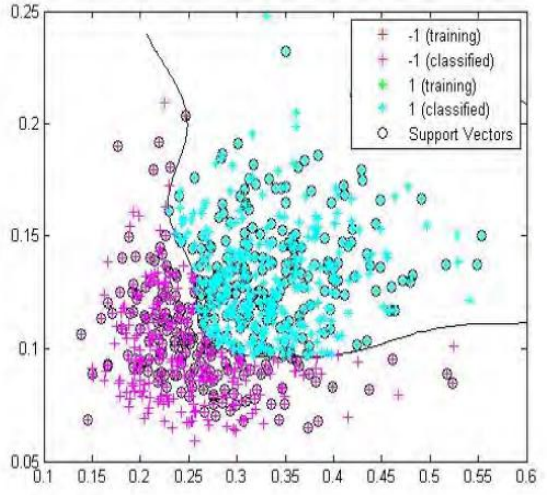

Fig.4 Identified speech samples between classes separated by decision boundary drawn by SVM

VI CONCLUSION

The characterization of sub-band entropies of speech spectrum for classifying female depressed patients and remitted subjects is proposed in this paper. Both analysis and experimental results showed that the studied entropies efficiently achieved in class separation with high correct classification percentages via SVM. More dynamic frequency sub-bands associated with the formant trajectory have to be reassigned for better performance of classification between diagnostic speech classes. The betterment in the result may be get by applying various algorithm and this work can be extended to detect exact speech features.

REFERENCES

[1] Asli Ozdas, Richard G. Shiavi, Senior Member, IEEE, Stephen E. Silverman, Marilyn K. Silverman, and D. Mitchell Wilkes, Member, IEEE. "Investigation of Vocal Jitter and Glottal Flow Spectrum as Possible Cues for Depression and Near-Term Suicidal Risk‖, *IEEE transactions on Engineering*, *Vol. 51, No. 9*, September 2004.

[2] Daniel J. France, Richard G. Shiavi, Senior Member, IEEE, Stephen Silverman, Marilyn Silverman, and D. Mitchell Wilkes, Member, IEEE. Acoustical Properties of Speech as Indicators of Depression and Suicidal Risk, *IEEE transactions on Engineering*, *Vol. 47, No.7*, July 2000.

[3] Hande Kaymaz Keskinpala, Thaweesak Yingthawornsuk, D. Mitch Wilkes, Richard G. Shiavi, and Ronald M. Salomon. Screening for High Risk Suicidal States Using Mel-Cepstral Coefficients and Energy in Frequency Bands. *15th European Signal Processing Conference (EUSIPCO 2007)*, Poznan, Poland, *September 3-7*, 2007.

[4] L. R. Rabiner , R. W. Schaber, *Digital processing of Speech Signals*. Prentice Hall.

[5] Thaweesak Yingthawornsuk. PhD Thesis.Acoustic Analysis Of *Vocal Output Characteristics For Suicidal Risk Assessment* Graduate School of Vanderbilt University, December, 2007.

[6] Digottex G., Glottal *source and vocal tract separation: Estimation of Glottal Parameters, Voice Transformation and Synthesis using a Glottal Model*, PhD, University Pierre and Marie Curie, December, 2010.

A Review on Transforms Involved in Digital Image Processing Technology

A.R.Agarawal[1],M.G.Vayada[2],V.H.Nayak[3]
[1]*PG Student, Department of Electronics & communication, L. D. College of Engineering, Ahmedabad, Gujarat, India*
[2]*Asst.Prof. Department of Electronics & communication, Silver Oak College of Engineering & Tecnology, Ahmedabad,Gujarat, India*
[3]*Asst.Prof. Department of Electronics & communication, Silver Oak College of Engineering & Technology, Ahmedabad,Gujarat, India*
[1]a.agrawal88@gmail.com,
[2]vayada.mohammed@gmail.com
[3]vimalhnayak@yahoo.com

***Abstract*- Transform theory plays a key role in image processing and will be applied during image enhancement, restoration etc. Many image processing algorithms are applied in the frequency domain rather than the spatial domain and transformation between the two domains can often permit more useful visualization of the image content. Transform theory is simply the transformation from one domain to another i.e. spatial to frequency domain. The present work is the study of various types of transforms involved in field of image processing.**

***Keywords*- Image Processing, Transform**

I INTRODUCTION

Image processing deals with analysis of images using different techniques. Image processing deals with the any action to change an image. Image processing has different methods like optical, analog and digital image processing. The computer algorithms can be modified so that we can also change the appearance of the digital image easily and quickly [1].

Digital image processing has fundamental classes which are grouped depending on their operations:

a. *Image enhancement:* image enhancement deals with contrast enhancement, spatial filtering, frequency domain filtering, edge enhancement and noise reduction. This project briefly shows the theoretical and practical approaches [1].

b. *Image restoration:* in this class the image is corrected using different correction methods like inverse filtering and feature extraction in order to restore an image to its original form [1].

c. *Image analysis:* image analysis deals with the statistical details of an image. Here it is possible to examine the information of an image in detail. This information helps in image restoration and enhancement. One of the representations of the information is the histogram representation to show the brightness and darkness in order to arrange and stretch the images to have an enhanced image relative to the original image [1].

d. *Image compression:* image compression deals with the compression of the size of the image so that it can easily be stored electronically. The compressed images are then decompressed to their original forms. Here the image compression and decompression can either lose their size by maintaining high quality or preserves the original data size without losing size [1].

e. *Image synthesis:* this class of digital image processing is well known nowadays in the film and game industry. Nowadays the film and game industry is very advanced in 3-dimensional and 4-dimensional productions. In both cases the images and videos scenes are constructed using certain techniques. The image synthesis has two forms tomography and visualization. [1].

Transform theory is simply the transformation from one domain to another .Transformation from spatial and frequency domain offers various advantages. Frequency domain offers some attractive advantages for image processing. It makes large filtering operations much faster, and it collects information together in different ways that can sometimes separate signal from noise or allow measurements that would be very difficult in spatial domain [2].

In case of spatial domain direct manipulation of pixels are possible. Spatial domain approach is very good for contrast enhancement. Also it is a good method for image sharpening. On the other hand in frequency domain, manipulation of frequency components is easier which can help for periodic noise removal. Also frequency domain approach is best suited for image sharpening [2].

The remainder of the paper is organized as follows. Section II describes various transforms involved in image processing such as Fourier transform, Discrete cosine transform, Wavelet transform and Curvelet transform , Section-III

describes experiments performed for each transform, Section-IV shown advantages and disadvantages of one transform over another and Finally conclusion and References.

II TRANSFORMS IN IMAGE PROCESSING

Transforms plays a key role in image processing and will be applied during image enhancement, restoration etc. The present section will give a brief introduction of various transforms involved in field of image processing such as fourier transform, discrete cosine transform, Wavelet transform and Curvelet transform .

Many image processing algorithms are applied in the frequency domain rather than the spatial domain and transformation between the two domains can often permit more useful visualization of the image content. Transform theory is simply the transformation from one domain to another i.e. spatial to frequency domain [4].

2.1 Fourier Transform

The image to be processed is transformed from spatial domain to frequency domain by the Fourier transform. After the needed frequencies removed it is easy to return back to the spatial domain [2].

The Fourier transform can be one dimensional or two dimensional depending on the variables in the spatial domain. In image processing two-dimensional Fourier transform is used. Before that it is good to define the Fourier transform. A Fourier transform is a representation of non-periodic functions as an integral of sine and cosine functions. In image processing the image is decomposed into sine and cosine components. Fourier transforms for one dimension can be represented below in the form

$$F(u) = \int_{-\infty}^{\infty} f(x) e^{-j2\pi ux} dx$$

The inverse Fourier transform can be represented by

$$f(u) = \int_{-\infty}^{\infty} f(x) e^{j2\pi ux} du$$

The above formulas can be extended for two dimensions as

$$F(u,v) = \int_{-\infty}^{\infty}\int_{-\infty}^{\infty} f(x,y) e^{-j2\pi(ux+vy)} dxdy$$

$$f(u,v) = \int_{-\infty}^{\infty}\int_{-\infty}^{\infty} f(x,y) e^{j2\pi(ux+vy)} dudv$$

2.2 Discrete Cosine Transform

The discrete cosine transform (DCT) helps separate the image into parts (or spectral sub-bands) of differing importance (with respect to the image's visual quality). The DCT is similar to the discrete Fourier transform: it transforms a signal or image from the spatial domain to the frequency domain [5].

The general equation for a 1D (*N* data items) DCT is defined by the following equation

$$F(u) = (\frac{2}{N})^{\frac{1}{2}} \sum_{i=0}^{N-1} A(i).\cos[\frac{\pi u}{2N}(2i+1)] f(i)$$

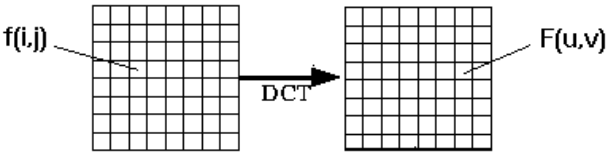

Fig.1 Direct Cosine Transform

and the corresponding *inverse* 1D DCT transform is simple $F^{I}(u)$, i.e.:

where $\Lambda(i) = \begin{cases} -\frac{1}{\sqrt{2}}, & for\ \xi = 0 \\ 1, & otherwise \end{cases}$

The general equation for a 2D (*N* by *M* image) DCT is defined by the following equation:

$$F(u,v) = (\frac{2}{N})^{\frac{1}{2}}(\frac{2}{M})^{\frac{1}{2}} \sum_{i=0}^{N-1}\sum_{j=0}^{M-1} \Lambda(i)\Lambda(j).\cos[\frac{\pi u}{2N}(2i+1)]\cos[\frac{\pi v}{2M}(2j+1)] f(i,j)$$

and the corresponding *inverse* 2D DCT transform is simple i.e.:

where $\Lambda(\xi) = \begin{cases} \frac{1}{\sqrt{2}}, & for\ \xi = 0 \\ 1, & otherwise \end{cases}$

2.3 Wavelet Transform

In mathematics, a wavelet series is a representation of a square-integrable (real- or complex-valued) function by a certain orthonormal series generated by a wavelet. This article provides a formal, mathematical definition of an orthonormal wavelet and of the integral wavelet transform [6].

The integral wavelet transform is the integral transform defined as

$$[W\psi f](a,b) = \frac{1}{\sqrt{|a|}} \int_{-\infty}^{\infty} \Psi\left(\frac{x-b}{a}\right) f(x) dx$$

The wavelet coefficients C_{jk} are then given by

$C_{jk} = [W\psi f](2^{-j}, k2^{-j})$

Here, $a=2^{-j}$ is called the binary dilation or dyadic dilation, and $b=k2^{-j}$ is the binary or dyadic position.

The wavelet transform has become a useful computational tool for a variety of signal and image processing applications [6].

Some algorithms for processing astronomical images, for example, are based on wavelet and wavelet-like transforms. One type of wavelet transform is designed to be easily reversible (invertible); that means the original signal can be easily recovered after it has been transformed. This kind of wavelet transform is used for image compression and cleaning (noise and blur reduction).

Typically, the wavelet transform of the image is first computed, the wavelet representation is then

modified appropriately, and then the wavelet transform is reversed (inverted) to obtain a new image.

The second type of wavelet transform is designed for signal analysis; for example, to detect faults in machinery from sensor measurements, to study EEG or other biomedical signals, to determine how the frequency content of a signal evolves over time. In these cases, a modified form of the original signal is not needed and the wavelet trans form need not be inverted (it can be done in principle, but requires a lot of computation time in comparison with the first type of wavelet transform).

The most basic wavelet transform is the Haar transform described by Alfred Haar in 1910. It serves as the prototypical wavelet transform. We will describe the (discrete) Haar transform with experimentation [6].

2.4 Curvelet Transform

Actually the ridgelet transform is the core spirite of the curvelet transform. In 1999, an anisotropic geometric wavelet transform, named **ridgelet transform**, was proposed by Candes and Donoho.

The ridgelet transform is optimal at representing straight-line singularities. Unfortunately, global straight-line singularities are rarely observed in ral applications. To analyze local line or curve singularities, a natural idea is to consider a partition of the image, and then to apply the ridgelet transform to the obtained sub-images. This block ridgelet-based transform, which is named curvelet transform, was first proposed by Candes and Donoho in 2000.

Apart from the blocking effect, however, the application of this so-called first generation curvelet transform is limited because the geometry of ridgelets is itself unclear, as they are not ture ridge functions in digital images. Later, a considerably simpler second-generation curvelet transform based on frequency partition technique was proposed. The second-generation curvelet transform has been shown to be a very efficient tool for many different applications in image processing. The overview of the curvelet transform is shown below for four step:

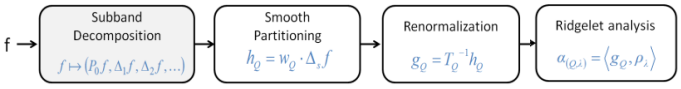

Fig.2 Steps involved in curvelet transform

Although the wavelet transform established an impressive reputation as a tool for signal processing, it has the disadvantage of poor directionality, which has undermined its usage in many applications. Significant progress in the development of directional wavelet has been made in recent years. In the necessary of anisotropic transform, a multiresolution geometric analysis, named curvelet transform was proposed.

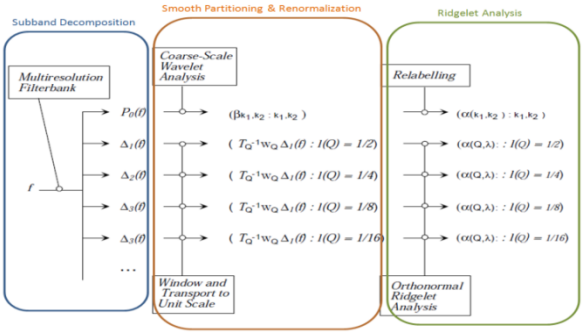

Fig.3 Overview of Organization of the Curvelet Transform

Being the extention of wavelet, it did make a impressive performance in image denoising and the result shows that it perform much better in image denoising and image enhancement.

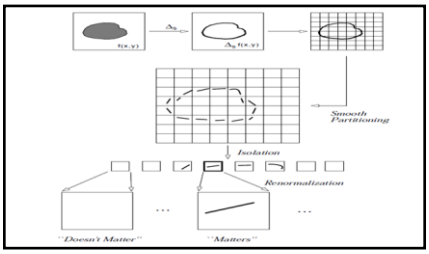

Fig.4 Spatial Decomposition of a Single Subband

III EXPERIMENTS PERFORMED WITH VARIOUS TRANSFORMS

3.1 Fourier Transform

A 1-D FT decomposes a signal into the sum of a set of sine/cosine waves. The output of the FT is the set of amplitudes and phases of these waves.

For image processing, we need the 2-D equivalent. The image is broken down into patterns which have a sinusoidal variation along each axis. We can display these patterns by taking the inverse FT of an array that is zero everywhere, except for a single value of 1. Thus we pick out a single Fourier component.

In the Fig, the component with M cycles on the y-axis and N cycles on the x-axis is at row M+1, column N+1.

Fig.5 Fourier components with M cycle on y & N cycles of x-axes

We read in an image, reduce the size, and display it. We make each dimension a number that has many small factors, as the Fast Fourier Transform algorithm can exploit this to speed up the calculation.

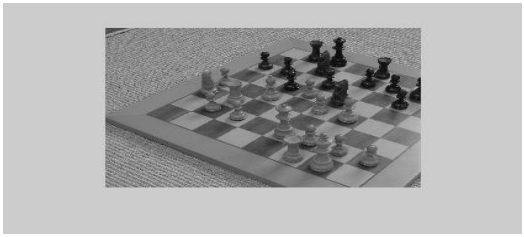

Fig.6 Displaying the image by reducing its size

We now compute the Fourier Transform of the image and display the amplitudes of the components. (That's what the call to abs gives.) We take the logarithm before display as otherwise the zero-frequency component dominates and we can't see any detail. The low-frequency components are at the corners of the plot and the high-frequencies are in the middle. There are two mirror symmetries, as mentioned earlier. The bright streak is a result of the high spatial frequencies in the carpet in the background.

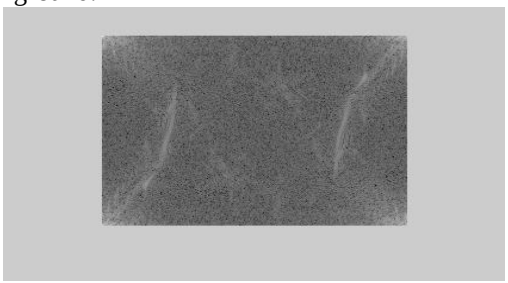

Fig.7 Fourier transform of image showing amplitudes of components

First we find the frequencies in units of "cycles across the image". This is what cxrange and cyrange are. Note that the frequencies become negative as we cross the centre of the image.

Then we convert to "radians per pixel", and store these as fxrange and fyrange. These are the correct units for mathematical manipulation of the FT. We use meshgrid to produce 2-D arrays containing the frequency values for every Fourier component.

Each of the components displayed in the first section is given the correct amplitude and phase for the chessboard image. Each image is made by adding together all the components with vertical frequency less than or equal to M, and horizontal frequency less than or equal to N, measured in cycles across the image. M and N depend on position in the display: they go 0, 1, 2, 4, 8 down the rows or across the columns. With 8 cycles in each direction, we have enough detail to see the squares on the chessboard.

We can suppress the high spatial frequencies by multiplying by an array that has large values only for the low spatial frequencies. Here, we do this by using a Gaussian function of the frequency. We display the logarithm of the mask, so that its structure is more visible.

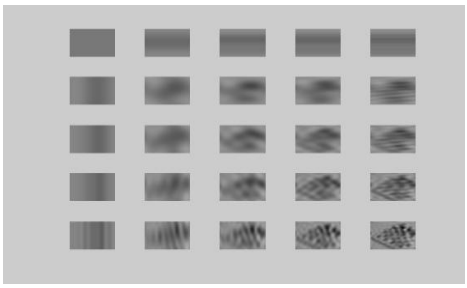

Fig.8 Reconstructed Image

We now simply multiply the FT point by point by this mask, and the take the inverse FT to get an image. The result is a smoothed image, because the higher spatial frequencies have been suppressed. In fact, it can be shown that this is equivalent to convolving the image with a Gaussian mask.

Fig.9 Image obtained by performing smoothing operation

We can perform other convolutions by multiplying the FT by a suitable mask. It turns out that multiplying by the x-frequency and also the imaginary unit i is equivalent to differentiating along the x-axis. (This doesn't work for the highest frequency, which has to be suppressed.)

This can also be understood as suppressing the low frequencies (on the x-axis) and emphasising the high frequencies, whilst preserving the symmetries of the FT.

As seen from the above experimentation. In the frequency domain the image enhancement deals with the frequency values manipulation. In the frequency domain the high or low frequencies are cut off depending on the result needed.

In this method a low-pass filter is used in order to remove noise. After removing the noise the image becomes blurred as in the same case as the spatial

ones. Therefore it is important to sharpen it using high pass filter to deal with the edges.

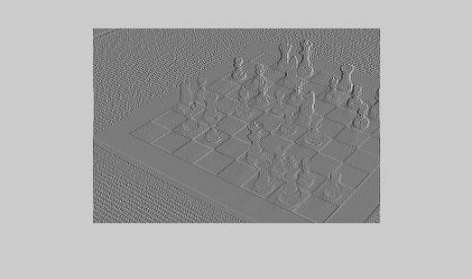

Fig.10 Image differentiation using fourier transform

3.2 Wavelet Transform

The Haar transform is the simplest orthogonal wavelet transform. It is computed by iterating difference and averaging between odd and even samples of the signal.To calculate the Haar transform of an array of *n* samples:

1. Find the average of each pair of samples. (*n*/2 averages)
2. Find the difference between each average and the samples it was calculated from. (*n*/2 differences)
3. Fill the first half of the array with averages.
4. Fill the second half of the array with differences.
5. Repeat the process on the first half of the array.

(The array length should be a power of two)

Two samples, *l* and *r*, can be expressed as an average, *a*, and a difference, *d*, like in mid-side coding:

$$a = (l + r) / 2$$
$$d = a - l = r - a$$

This is reversible:

$$l = a - d$$
$$r = a + d$$

Since we are in 2-D, we need to compute the average and difference in the horizontal and then in the vertical direction (or in the reverse order, it does not mind).

3.3 Curvelet Transform

We can discover that the curvelet transform is the best than other method. The reconstruct image by curvelet will not cause artifact along the edge. But there still some disadvantage that the ridgelet transform will cause "wrap around".Curvelet can also be utilized for image enhancement The approch of image enhancement is describe as follow: First, apply the curvelet transform to the image. Then,accroding to noise ratio of each subband, enforce sectional nonlinear enhancement to the coefficients. At last, apply the inverse curvelet transform to the coefficients and come out the image with image enhancement on edge.

IV CONCLUSION

The Fourier Transform is an important image processing tool which is used to decompose an image into its sine and cosine components. The output of the transformation represents the image in the *Fourier* or frequency domain, while the input image is the spatial domain equivalent.

The wavelet transform is useful for the compression of digital image files; smaller files are important for storing images using less memory and for transmitting images faster and more reliably.

When it come to the application of curvelet transform, it is divided into three main parts :

(1) Image denoising
(2) Image enhancement
(3) Compressed Sensing

Lots of experiments have been to compare the wavelet transform and curvelet transform in different application. It is shown that the curvelet transform is able to reach better performance than the wavelet transform in above three applications.

At last, as curvelet transform is not a fully mature technology because it is just proposed in a decade, I conclude two direction of future work for nowadays curvelet: (1) Reducing complexity (2) Better thresholding function.

REFERENCES

[1] Rafael Gonzalez and Richard E. Woods. Digital Image Processing. Addison-Wesley, second edition, 2002.

[2] The Math Works, Inc. [online].Pixel representation; 1984-2011. URL:http://www.mathworks.com/help/toolbox/images/brcu_al-1.html Accessed January 2011.

[3] Ming Zhang . Bilateral Filter Image Processing. Louisiana State University; 2009

[4] Jerry Lordriguss. Digital image processing;1974-2010. URL: http://www.astropix.com/HTML/J_DIGIT/TOC_DIG.HTM . Accessed January 2011.

[5] Trees image; copyright Susan Cohen; The Math Works, Inc. MATLAB software; 1984-2010.

[6] Arash Abadpour. Color Image Processing Using Principal Component Analysis. Tehran Iran, SHARIF University of Technology ; 2005.

TM

SOCET

Silver Oak College of Engineering & Technology

WE THINK ABOUT YOUR FUTURE

Silver Oak College of Engineering & Technology

352, 353 A, NEAR BHAVIK PUBLICATIONS,
OPPOSITE BHAGWAT VIDHYAPITH,
GOTA CROSS ROAD, AHMEDABAD-382481.

ISSN : 2320 - 2122